SYNTHESIS, CHARACTERIZATION, AND GELATION AND DEVELOPMENT OF LIQUID CRYSTALLINE ORDER DURING ISOTHERMAL CURE OF RIGID ROD EPOXY

By

SEUNGHYUN CHO

A DISSERTATION PRESENTED TO THE GRADUATE SCHOOL
OF THE UNIVERSITY OF FLORIDA IN PARTIAL FULFILLMENT
OF THE REQUIREMENTS FOR THE DEGREE OF
DOCTOR OF PHILOSOPHY

UNIVERSITY OF FLORIDA

2002

This work is dedicated to my family: my mother, father and sister for their love, support and trust in me; my husband, Dr. Bongsoo Lee; and my children, Chungwon and Suyeon for their love and patience. Without their endless caring and support, this work would not have been possible.

ACKNOWLEDGMENTS

I would first like to acknowledge my advisor, Dr. Elliot P. Douglas, for his support, encouragement, knowledge and guidance. I also appreciate the members of my supervisory committee: Dr. Ronald Baney, Dr. Randolph Duran, Dr. Laurie Gower and Dr. Wolfgang Sigmund for their valuable advice and guidance.

I would like to extend my gratitude to my colleagues: Dr. Arthur Gavrin for his helpful knowledge and support in synthesis, Dr. Jianxun Feng and Dongsik Kim for their kind and friendly advice and encouragement. I also thank all of my group members and friends who gave support, collaboration and encouragement: Yi-yeoun Kim, Tonya Bervaldi, Wei-ling Jia, Susan Leander, Stephanie DiFrancesco, Elizabeth Oborn, Dr. Han-ying Zhao and Derek Lincoln.

I greatly appreciate the provider of funding for this project: the U.S. Army Research Office (under Grant DAAG55-98-1-0114 to Dr. Elliot P. Douglas as a Presidential Early Career Award for Scientists and Engineers).

TABLE OF CONTENTS

page

ACKNOWLEDGMENTS.....ii

LIST OF TABLES.....vi

LIST OF FIGURES.....vii

ABSTRACT.....ix

CHAPTER

1 REVIEW OF LITERATURE.....1

1.1 Liquid Crystals.....1
1.1.1 Liquid Crystalline Polymers (LCPs).....3
1.1.2 Liquid Crystalline Thermosets (LCTs).....4
1.1.3 Applications.....6
1.2 Thermal Stability.....8
1.3 The Transition Diagrams.....9
1.3.1 Gelation and Vitrification Times.....9
1.3.2 Measurements of Transitions.....10
1.3.3 Transition Diagrams.....11
1.4 Curing Kinetics.....13
1.5 Goals of This Study.....15

2 SYNTHESIS AND CHARACTERIZATION OF LIQUID CRYSTALLINE EPOXY MONOMERS.....17

2.1 Introduction.....17
2.2 Experimental Section.....18
2.2.1 Synthesis of 4,4'-diglycidyloxy-α-methylstilbene (DOMS).....18
2.2.2 Synthesis of D2A1.....22
2.2.3 Thermogravimetric Analysis (TGA).....24
2.2.4 Results and Discussion.....24
2.2.5 Synthesis of DOMS.....24
2.2.6 Synthesis of D2A1.....37
2.2.7 Thermal Analysis.....43
2.3 Other Syntheses.....58

1.1.1 Synthesis of Compound II with Hydroquinone Started from Allyl Bromide.....58
1.1.2 Compound III with Methoxy Hydroquinone.....61
1.1.3 Compound IV with Biphenol.....62
1.1.4 Synthesis of Compound VI with Hydroquinone Started from 8-Bromo-1-Octene.....63
1.1.5 Synthesis of Compound VII.....64
1.1.6 Synthesis of Compound VIII with Acetoxy Benzoic Acid.....65
1.2 Conclusions.....67

2 GELATION AND DEVELOPMENT OF LIQUID CRYSTALLINE ORDER DURING ISOTHERMAL CURE OF RIGID ROD EPOXY.....69

2.1 Introduction.....69
2.2 Experimental Section.....70
2.2.1 Materials and Sample Preparation.....70
2.2.2 Parallel Plate Rheology.....71
2.2.3 Differential Scanning Calorimetry (DSC).....71
2.3 Results and Discussion.....72
2.3.1 Transition Diagrams.....72
2.3.2 Gel Points vs. Conversion.....82
2.3.3 Phase Transition vs. Conversion.....88
2.4 Conclusions.....93

3 CONCLUSIONS AND FUTURE WORK.....95

REFERENCES.....102

BIOGRAPHICAL SKETCH.....109

LIST OF TABLES

Table page

2-1 Elemental Analysis results for diol.....19

2-2 Elemental Analysis results for DOMS.....20

2-3 Elemental Analysis results for D2A1.....23

2-4 Transition temperatures of DOMS.....31

2-5 Transition temperatures of D2A1.....38

2-6 Gelation times for various curing agents.....43

2-7 Thermogravimetric Analysis data comparison for DOMS and DGEBA.....50

2-8 Elemental Analysis results of Compound I.....60

2-9 Elemental Analysis results of Compound II.....60

2-10 Transition temperatures (10°C/min rate).....61

2-11 Elemental Analysis results of Compound III.....62

2-12 Elemental Analysis results of Compound IV.....62

2-13 Transition temperatures (10°C/min rate) of Compound IV.....62

2-14 Elemental Analysis results of Compound V.....63

2-15 Elemental Analysis results of Compound VI.....64

3-1 Times of liquid crystalline phase appearance by POM (t_{lc}) and second peak maximum of DSC (t_{peak}).....78

3-2 Gel times and conversion at gel points.....88

3-3 Times of liquid crystalline phase appearance (t_{lc}) and conversion at phase transition (α_{lc}).....91

LIST OF FIGURES

Figure page

1-1 Liquid crystalline mesophases....2

1-2 Typical LCT monomers....7

2-1 Synthesis scheme for Diol....26

2-2 Synthesis scheme for DOMS....27

2-3 Synthesis mechanism for Diol....29

2-4 Synthesis steps of DOMS from diol and epichlorohydrin....30

2-5 DSC thermographs for DOMS (10°C/min, N_2)....32

2-6 Scheme of DOMS and sulfanilamide....34

2-7 Curing mechanism....35

2-8 Synthesis scheme for D2A1....39

2-9 Polarized optical microscopy of D2A1....40

2-10 Curing agents....44

2-11 Gel point and vitrification point determination....45

2-12 Thermogravimetric Analysis scan of DOMS-SAA system (heating rate 10°C/min, under N_2)....46

2-14 Chemical structure of DGEBA....48

2-15 Thermogravimetric Analysis scan of DOMS and DGEBA (heating rate 10°C/min, under N_2)....48

2-16 Thermogravimetric Analysis scan of D2A1-2.0wt%MI system....49

2-17 Flynn-Wall plot of DOMS-SAA system.....53

2-18 Plot of ln q vs. 1/T for α=0.40 for calculation of E_d.....54

2-19 Activation energies for decomposition of DOMS-SAA system.....55

2-20 Activation energies for decomposition of D2A1-2.0wt% MI system.....56

2-21 Synthesis scheme.....59

2-22 Molecular structure of Compound III.....61

2-23 Molecular structure of Compound IV.....62

2-24 Molecular structure of Compound VI.....64

2-25 Synthesis scheme.....65

2-26 Synthesis scheme.....66

3-1 Liquid Crystalline Phase Time Temperature Transformation diagram of DOMS-SAA system.....75

3-2 Isothermal scan diagram of DSC at 150°C.....77

3-3 Time Temperature Transformation diagram of D2A1-1.5 wt% MI system.....79

3-4 Liquid Crystalline Phase Time Temperature Transformation diagram of D2A1-2.0wt% MI system.....80

3-5 Time Temperature Transformation diagram of D2A1-2.5 wt% MI system.....81

3-6 Cure exotherm of uncured and partially cured sample.....84

3-7 Conversion at gelation for DOMS-SAA system.....87

3-8 Arrhenius plot of ln (t_{gel}) vs. 1/T.....89

3-9 Plot of phase transition temperature and gel points vs. conversion.....90

3-10 Idealized plot for cure temperature vs. time or conversion.....100

Abstract of Dissertation Presented to the Graduate School
of the University of Florida in Partial Fulfillment of the
Requirements for the Degree of Doctor of Philosophy

SYNTHESIS, CHARACTERIZATION, AND GELATION AND DEVELOPMENT OF LIQUID CRYSTALLINE ORDER DURING ISOTHERMAL CURE OF RIGID ROD EPOXY

By

Seunghyun Cho

August 2002

Chairman: Elliot P. Douglas
Major Department: Materials Science and Engineering

The liquid crystalline thermoset monomers 4,4'-diglycidyloxy-α-methylstilbene (DOMS) and D2A1 that resulted from reaction between DOMS and aniline were synthesized. The monomers were characterized with cross-polarized optical microscopy, differential scanning calorimetry (DSC) and dynamic thermogravimetric analysis (TGA). DOMS showed monotropic liquid crystalline mesophase and D2A1 showed smectic phase even at room temperature and turned into nematic then cleared upon heating.

DOMS was cured with sulfanilamide (SAA) and D2A1 was cured with catalytic curing agent, 1-methyl imidazole (MI). Thermal stability tests of DOMS-SAA, D2A1-MI and commercial nonliquid crystalline epoxy, diglycidyl ether of bisphenol A (DGEBA) SAA system via dynamic TGA shows that the factor that most influences thermal stability is the molecular structure of the material itself rather than liquid crystalline phases. The %conversion data were determined from dynamic DSC scan to examine the

applicability of Flory's gelation theory. The results reveal that even though the amount of reaction that occurs in the liquid crystalline phase is different at different cure temperatures, the isoconversion theory of gelation fits quite well. The actual average value of the conversion at the gel point is 0.677, which is slightly higher than the calculated theoretical value of 0.577 because of the failed assumptions of this theory. That is, there might be reactivity differences among the same types of functional groups and intramolecular connections are possible.

The phase transitions do not show isoconversion behavior in contrast to gelation. Instead, the conversion where phase changes from isotropic to a liquid crystalline phase tends to increase with temperature because the critical length of the molecules needed for the liquid crystallinity increases with temperature.

CHAPTER 1
REVIEW OF LITERATURE

1.1 Liquid Crystals

Liquid crystals, discovered in 1888, are substances that exhibit long-range orientational order and either zero-, one-, or two-dimensional position order (de Gennes 1974). Therefore the liquid crystals are in-between in properties while crystalline materials have three-dimensional, long-range order and amorphous substances are somewhat entirely disordered (Sperling 1992). Compared to anisotropic states in which the properties vary in different directions, the substances that possess the same properties in all directions and have no long-range order in any direction are called isotropic. The liquid crystals show an in-between state, and show intermediate forms of phases called mesomorphic phases. The main cause for the formation of liquid crystals is molecular asymmetry and is due to intermolecular repulsion, i.e., the fact that two molecules cannot occupy the same space at the same time.

Figure 1-1 shows some liquid crystalline mesophases. The nematic liquid crystals have long-range orientational order and zero-dimensional long-range positional order. The smectic liquid crystals have long-range orientational order and one-dimensional long-range positional order. Smectic liquid crystals are known to be more viscous than nematic liquid crystals if everything else is the same. The discotic liquid crystals (which look like stacks of discs) have two-dimensional positional order. The cholesteric liquid crystals form layers, and look like a two-dimensional twisted nematic mesophase.

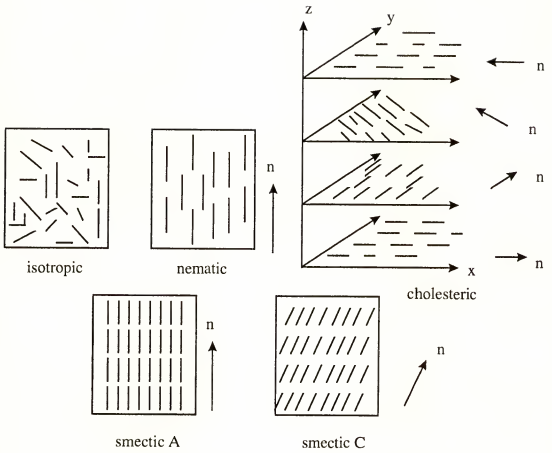

Figure 1-1 Liquid crystalline mesophases

The liquid crystals may exhibit multiple mesophases at different temperatures or pressure, and the mesomorphic transitions are first-order transitions rather than second-order since heat capacity and volume show discontinuity when plotted against temperature or pressure (Sperling 1992).

Other classifications of liquid crystals by mesophase structure are lyotropic and thermotropic. The lyotropic liquid crystals exhibit liquid crystallinity in concentrated solutions. The lyotropic liquid crystals can become isotropic by heating or adding more solvent. Thermotropic liquid crystals exhibit liquid crystallinity upon melting. They exhibit the flow behavior of isotropic liquids but possess some long-range order. By heating the thermotropic liquid crystals, they transform into an isotropic liquid state at a temperature called the liquid crystal-isotropic phase transformation temperature. Both lyotropic and thermotropic liquid crystals appear turbid and become clear when isotropic.

For nematic and smectic liquid crystals, although no methods predict with certainty whether a given molecule will show liquid crystallinity, an elongated molecule is usually needed (typically made from rigid rod-like segments, often with flexible tails). Rigid-rod liquid crystals have rigid groups either in the polymer chains, called main chain liquid crystals or as side groups of the polymer chains, called side chain liquid crystals. Theses rigid groups are called mesogens or mesogenic groups.

1.1.1 Liquid Crystalline Polymers (LCPs)

Although liquid crystalline behavior has been known for more than 100 years, liquid crystalline polymers (LCPs) have attained prominence relatively recently. LCPs have many desirable characteristics for use as structural polymers, such as excellent dimensional stability, good mechanical properties in the direction of orientation, low

thermal expansion, and good high temperature properties (Noel and Navaro 1991).

Studies focused on liquid crystalline polymers emerged because of the discovery of aramids (poly p-phenyleneterephthalamide) and thermotropic polyesters, and the commercial development of strong fibers and plastics from these materials. The aramids are spin-processed into fibers by using lyotropic solutions in sulfuric acid. Because of the high melting point of LCPs, they cannot be melt-processed. LCPs have practical advantages such as the followings:

- They have lower viscosities which make them easier to process than melts or solution of random-coil polymers
- They can be oriented during processing and yield high strength and high modulus
- The strength and moduli are considerably higher than chain-folded crystalline polymers obtained from non-liquid crystalline polymers (Odian 1991).

However, their high melting point is a major barrier for processing.

1.1.2 Liquid Crystalline Thermosets (LCTs)

Disadvantages of LCPs (such as their relatively high cost and high temperature for processing) turned researchers' attention to liquid crystalline thermosets (LCTs) (Douglas et al. 1994, Shiota 1997a, Körner et al. 1996a). LCTs are defined as low molecular mass liquid crystals with functional end groups attached (Hoyt et al. 1989), that can be crosslinked thermally, chemically, or photochemically locking in liquid-crystalline order. The schematic of a typical monomer is shown in Figure 1-2. As we can see from the figure, these molecules are normally made from rigid rod-like segments with crosslinking groups attached to flexible segments. The advantageous properties of LCTs include good mechanical properties and chemical resistance, low shrinkage on curing, higher fracture toughness than conventional thermosets, and the ability to orient their

molecules under the influence of mechanical, electric or magnetic fields (Douglas et al. 1994, Shiota et al. 1997a, Körner et al.1996a, Hoyt et al. 1989, Lincoln and Douglas 1999, Melissaris and Litt 1994, Litt et al. 1993). Their low viscosity during the initial stage of processing makes it possible to fill complicated molds easily or thoroughly penetrate fiber weaves or mats for the formation of fiber composites. Many researchers have attempted to synthesize LCT monomers with acrylate and methacrylate (Litt et al. 1993, Hikmet and Broer 1991), acetylene (Langlois et al. 1998, Melissaris and Litt 1994, Benicewicz et al. 1997a), epoxy (Domszy and Shannon 1990, Mallon and Adams 1993), maleimide or nadimide (Hoyt and Benicewicz 1990a, Hoyt and Benicewicz 1990b), vinyl functional groups (Hikmet et al. 1993) and cyanate ester (Körner et al. 1996b) functional groups.

Among these LCTs, liquid crystalline epoxies (LCEs) have been studied intensively since liquid crystalline (LC) epoxy networks were patented in the mid 1980s and many studies have been done on LC epoxy systems consisting of rigid-rod monomers crosslinked with a variety of reagents (Amendola et al. 1996, Barclay et al. 1992b, Barclay et al. 1992a, Giamberini et al. 1995b, Lee and James 1998, Lee et al. 1998, Liu et al. 1996, Liu et al. 1997, Mallon and Adams 1993, Noel and Navard 1991, Su 1993). One of the LCEs which has been focused on recently by many researchers is the diglycidyl ether of 4,4'-dihydroxy-α-methylstilbene, or 4,4'-diglycidyloxy-α-methylstilbene (DOMS) (Barclay 1992a, Barclay 1992b, Carfagna 1993, Earls 1992, Lin 1994, Amendola 1995, Giamberini 1995b, Amendola 1996, Lin 1997). They studied synthesis, mechanical and magnetic alignment, curing reactions with various curing agents and curing kinetics. The fracture toughness is known to be higher especially in the smectic

liquid crystalline state than in the isotropic state of the same LCE (Carfagna et al. 1994, Ortiz et al. 1998a, Ortiz et al. 2000), since the smectic LCTs exhibited highest fracture toughness due to bulk, homogeneous plastic yielding. The isotropic, non-LC based thermoset exhibited catastrophic, brittle failure and very low fracture toughness.

Ortiz et al. (1998a) concluded that the isolated fracture of individual domains producing microscopic defects and voids near the crack tip resulted in the high toughness of smectic LC phase. Also even in same liquid crystalline phase, the domain sizes are different at different curing temperatures and this affects the fracture toughness of the materials. The LCE cured by gradually raising the temperature had larger and more perfect LC domains with defects or low molecular weight species around the inter-LC domain region, which allowed the crack to propagate along the inter-LC domain region. Therefore the LCE cured with sufficient time showed lower fracture toughness than the LCE cured with limited time in which the size of the smectic LC domains was smaller and less perfect (Sue et al. 1997). Liu et al. (1996) examined the influence of thermal history on the properties of the LCE system and found that LC domain size, degree of liquid crystallinity and thermal properties varied with the reaction temperature. Barclay et al. (1992a) synthesized the LC epoxy oligomer and found that the lower molecular weight and the narrow dispersity of oligomers cured resulted in networks with smectic-like structure due to the regular distance between crosslink sites even though the parent prepolymer showed nematic LC phase.

1.1.3 Applications

Liquid crystalline materials have many applications in various fields. One of the most important applications is when fabricating ultra-high strength materials.

For example, high-modulus Kevlar aramid fibers have been used for rubber reinforcement in tires and belts, for ropes and cables, for pressure-wound vessels such as rocket engine cases and for protective clothing such as bullet-resistant vests. Also it has been used alone or with glass and carbon fiber in various composite applications such as aircraft panels, flooring, race-car bodies and sporting goods. Highly oriented LCP films with mesogenic side chains can be used for information-storage devices (Enc 1986).

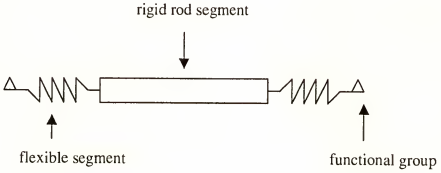

Figure 1-2 Typical LCT monomer

LCTs find applications in fields in which conventional thermosetting materials have been used, such as composites where the resins act as high rigid networks and matrices for advanced material (in automobiles and aerospace industries or adhesives, coatings, electronic packaging, LC displays and nonlinear optics). Polymer dispersed liquid crystals (PDLC) with micron-sized liquid crystalline droplets imbedded in a transparent polymer matrix are applicable for optical switches, light valves, filters, shutters, information displays and many transmittance windows, because they can be controlled electrically and switched between relatively translucent (light scattering) and relatively transparent (light transmitting) states.

1.2 Thermal Stability

The structure-sensitive transition temperatures (such as the glass transition temperature, crystalline melting temperature and heat degradation temperature) are often used to characterize and understand thermal properties and to determine the temperature range and thermal resistance of polymeric materials. Thermal decomposition characteristics are used to estimate the properties needed for a high performance and heat resistance matrix (Lee et al. 2001). Heat resistance is generally evaluated using thermogravimetric analysis (TGA), isothermogravimetric analysis (ITGA), and differential scanning calorimetry (DSC) (Nam and Seferis 1991, Scariah et al. 1994, Dyakonov et al. 1996, Frich and Economy 1997, Lee et al. 2001, Liu et al. 1998). Results can be affected by sample formation, heating rate, thermal history, and atmosphere. For example, samples of powder form lose more weight than films because of higher surface area. Also if the heating rate is higher, the apparent thermal stability is higher. Normally, the data obtained from TGA are analyzed by the calculation of activation energies for decomposition (Nam and Seferis 1991, Dyakonov et al. 1996, Lee et al. 2001, Lu et al. 2000).

Generally, thermal degradation does not occur until the temperature reaches a level where the primary chemical bonds are dissociated. For many materials, thermal degradation is characterized by breakage of the weakest bond and determined by bond-dissociation energy. Therefore the effect of structure on thermal stability has been studied (Gouri et al. 2002, Oprea 2002, Yang 2002).

However study of thermal stability of liquid crystalline materials, especially of LCTs is rare. Lam et al. (2000) found an increase of the thermal decomposition

temperature with increasing spacer length for LC polyacetylenes. It is known that liquid crystalline materials with aromatic repeat units have good thermal resistance. Gavrin et al. (1999) showed LCTs with phenylethynyl group had onset of weight loss at 423°C in nitrogen and 397°C in air atmosphere. Lu et al. (2000) studied the influence of types of hardener and showed lower thermal stability when cured with a curing agent contained an aliphatic linkage. Also as the mesogen concentrations of curing agents increased, the decomposition temperatures increased (Farren et al. 2001).

Thermal stabilities of LCPs containing imides (Hsu et al. 1998, Pramoda et al. 2000) and LC polyacetylenes (Lam et al. 2000) have been presented. Frich and Economy (1997) showed an LCT based on all aromatic ester units is thermally stable to 450°C by 5% weight loss. However studies comparing the thermal stability of the different phases of the same LC are rare. Therefore our study compares the thermal degradation paths of the same LCTs at different phases.

1.3 The Transition Diagrams

1.3.1 Gelation and Vitrification Times

Gelation is considered as the point of an infinite molecular network and infinite viscosity, which causes viscoelastic behavior in the macroscopic fluid. Before gelation occurs, the polymer chains grow and branch in the soluble and fusible liquid state. As the cure proceeds, the viscosity of the system increases due to the increase of molecular weight, an infinite network of polymer chains develops, and the reaction becomes diffusion-controlled from kinetically controlled and vitrifies. Vitrification points are when the glass transition temperature is equal to the isothermal cure temperature. Vitrification involves transformation of a material from a liquid or rubbery state to a

glassy state as a result of an increased molecular weight. Near these points, kinetics are affected by local viscosity, and therefore the cessation of reaction might be due to quenching caused by vitrification rather than the completion of the reaction.

Many methods such as thermal mechanical analysis (TMA), dynamic mechanical thermal analysis (DMTA), differential scanning calorimetry (DSC), solubility tests, torsional braid analysis (TBA), and rheological measurements have been used to determine gelation and vitrification, as well as rheological behavior (Ampudia et al. 1999, Cadenato et al. 1997, DeMeuse et al. 1997, Gillham and Enns 1994, Jahromi et al. 1995, Lange et al. 2000, Laza et al. 1998, Mauri et al. 1996, Nunez et al. 1997, Nunez et al. 1998, Simon et al. 1992, Wang and Gillham 1993, Wisanrakkit and Gillham 1990, Zukas 1994).

Several methods have been used to determine the gel points of LCTs. Shiota et al. (1997b) evaluated the gel point of an LC dicyanate as a crossover point of G' and G" via rheological measurements. Jahromi et al. (1995) confirmed that the gel points of an LC diepoxide determined from rheological measurements and solubility experiments are the same.

1.3.2 Measurements of Transitions

Physical transitions. To investigate the response of a material to rapid processes or to examine transitions, dynamic methods are needed. Cyclic motion is given to a specimen and the resultant response is measured. Dynamic techniques determine the storage modulus, G', loss modulus, G", and the loss tangent, tan δ. The measurements are performed as a function of temperature, time, or frequency and the results are used in determining transitions, chemical reactions and properties (Enc 1986). Rheological

devices and techniques have been used to determine gel and vitrification points or kinetics. (Ampudia et al. 1999, Jahromi et al. 1995, Laza et al. 1998)

Liquid crystalline phase transitions. Liquid crystalline phase changes are normally observed by cross-polarized optical microscopy and differential scanning calorimetry (Percec et al. 1991, Carfagna et al. 1993, Mallon et al. 1993, Ogawa 1996, Ochi et al. 1997, Gavrin et al. 1999) Ochi et al. (1997) presented the effect of different crosslinking agents on an LCE, which did not show liquid crystallinity as a monomer but developed Schlieren texture with a certain crosslinking agent as curing proceeded because the mesogenic groups in the system were ordered as curing proceeded. This result also appeared in the DOMS monomer. (Liu 1997)

1.3.3 Transition Diagrams

The curing of thermosetting materials can be expressed in terms of cure-property diagrams such as the conversion-temperature-property (T_gTP) diagram (Wang and Gillham 1993), the glass transition temperature (T_g) vs. conversion diagram (Wisanrakkit and Gillham 1990), the continuous heating transformation (CHT) cure diagram (DeMeuse et al. 1997), and the time-temperature-transformation (TTT) isothermal cure diagram (Gillham and Enns 1994, Simon et al. 1992, DeMeuse et al. 1997). The T_gTP diagram deals with the relationship between the material properties and the extent of cure during isothermal cure. Wisanrakkit and Gillham (1990) developed T_g as an index of chemical conversion by a model study of an epoxy cured with an amine. The CHT cure diagram is obtained via heating the unreacted mixture from below its initial glass transition temperature to above its maximum glass transition temperature at different heating rates. Temperature is plotted on the y-axis, with log time plotted

on x-axis. One specimen is examined for each heating rate.

TTT diagram is constructed by measuring the times to the events of interest, such as gelation, vitrification, full cure, and devitrification (Enns and Gillham 1983). Cure temperature T_{cure} is plotted on the y-axis and log time on the x-axis. Again one specimen is examined for each isothermal temperature. The gelation contour and S-shaped vitrification curves in a TTT diagram divide the diagram into the characteristic states of the thermosetting cure process, such as liquid, sol/gel rubber, elastomer (gel rubber), ungelled glass (sol glass), gelled glass and char. In the TTT diagram, the important three temperatures are T_{go}, $_{gel}T_g$, and $T_{g\infty}$. T_{go} is the temperature below which no significant reaction of the mixture of epoxy and curing agent occurs (Nunez et al. 1997). This temperature might also be considered as the storage temperature for an uncured resin mixture because the reaction is too slow to be considered significant. If T_{go} < room temperature, the uncured sol mixture is a liquid at room temperature, and if T_{go} > room temperature, the uncured sol mixture is a glassy solid at room temperature that upon heating will flow and react. In an ideal case, gelation and vitrification occur at the same time and $_{gel}T_g$ is the temperature where this phenomenon occurs. If $_{gel}T_g$ > storage temperature, then even though the material reacts and solidifies during storage, it remains sol and flows on heating and still processible, and if $_{gel}T_g$ < storage temperature, the material gels before it solidifies. $T_{g\infty}$ is the cure temperature where the degree of conversion reaches its maximum (i.e. =1). However it is impossible to reach this value experimentally.

Transition diagrams also have been constructed for LCTs. Schematic phase diagrams for the general melting behavior of LCTs, (Hoyt and Benicewicz 1990b,

Benicewicz et al. 1997a) an experimentally determined non-equilibrium phase diagram (Langlois 1998), a process characterization diagram (Mallon and Adams 1993) and time-temperature-phase transformation diagrams (Lin et al. 1994, Shiota et al. 1997a) are examples. The schematic phase diagrams plot temperature vs. extent of reaction during isothermal cure, giving information about phase transitions only. Since the experimentally determined transformation diagram is based on one cure temperature, the information about the liquid crystalline phase changes as well as the physical transformations at different cure temperatures cannot be obtained.

The time-temperature-phase transformation diagram represents the LC phase changes during isothermal cure by plotting temperature vs. time and gives no physical transformation, either. A new liquid crystalline phase-time-temperature-transformation (LCPTTT) diagram (Gavrin and Douglas 2001) is constructed for LCTs and gives information about liquid crystalline phase changes as well as physical transformations during isothermal cure. In this study new LCPTTT diagrams will be constructed for the LCT system studied to give important information needed for processing.

1.4 Curing Kinetics

Epoxy resins have been investigated from many ways because of their applications in various ways. Because a precise understanding of curing kinetics is one of the most important factors for practical models and basic theory, there has been many studies on curing kinetics and mechanisms of LC epoxies as well as non-LC epoxies (Carfagna et al. 1993, Liaw et al. 1994, Liu et al. 1997, Liu et al. 1998, Matejka 2000, Micco et al. 1997, Ooi et al. 2000, Ricciardi et al. 1983, Tatsumiya et al. 1997).

The curing process may play an important role in liquid crystalline phase formation and in determining the final crosslinked structures of conventional thermosets. Carfagna et al. (1993) presented curing kinetics of the DOMS with different curing agents, one could be crosslinked in an LC phase, and the other in a non-LC phase. They found the major reason of non-LC phase formation to be predominance of intramolecular hydrogen bonding of this crosslinking agent. Intramolecular hydrogen bonding made a growing prepolymer folded, which is opposing to formation of LC phase. Amendola et al. (1995) examined kinetics of second exothermic appeared in isothermal DSC spectra of DOMS-diaminotoluene system. They showed there're relations between the onset of second peak and transition from isotropic to LC phase.

Theoretical analysis of gelation vs. conversion

Applying Flory and Stockmayer's theory and statistical approach (Flory 1953, Stockmayer 1951), the extent of reaction at gel point is expressed by Cadenato et al. (1997) in the following equations of,

$$\alpha_{E_g} = \left[\frac{m_A f_A}{m_E f_E (f_A - 1)(f_E - 1)} \right]^{\frac{1}{2}}$$

$$\alpha_{A_g} = \left[\frac{m_E f_E}{m_A f_A (f_A - 1)(f_E - 1)} \right]^{\frac{1}{2}}$$

where α_{Eg} is the fraction of the epoxy group reacted at the gel point,
m_E is the number of moles of epoxy component,
f_E is the functionality of the epoxy component used,
α_{Ag} is the fraction of the amine group reacted at the gel point,
m_A is the number of moles of amine component,
and f_A is the functionality of the amine component used

When stoichiometric amounts are used for both components, both previous equations can be expressed with functionality only

$$\alpha_{A_g} = \alpha_{E_g} = \alpha_g = \left[\frac{1}{(f_A - 1)(f_E - 1)}\right]^{\frac{1}{2}}$$

where α_g is the extent of reaction at the gel point.

For this theory there are two main assumptions: all functional groups have equal reactivity; ring formation does not occur in molecular species of finite size. However the second assumption is never correct in real systems and causes considerable error in calculations. Using effective functionalities less than the true stoichiometry may reduce those errors. This theory has been proven experimentally for conventional thermoset systems. (Cadenato et al. 1997, Nunez et al. 1997) However, the experimental results regarding LCTs are rare. Therefore in this study we examined whether the gelation theory holds for the liquid crystalline epoxy systems.

1.5 Goals of This Study

There are three main goals for this study. The first is to synthesize and characterize LCT monomers. One is a well-known LCT (DOMS); and the other is a new LCT (D2A1). For the characterization, LCT monomers have been studied using cross-polarized optical microscopy, differential scanning calorimetry, and thermogravimetric analysis. In the thermal degradation study, the important factors that influence thermal stability have been emphasized.

The second goal is to construct liquid crystalline phase-time-temperature-transformation diagrams, which allow us to determine liquid crystalline phase transition times as well as physical transformation times during isothermal cure. The physical

transition times and liquid crystalline phase transition times are determined from parallel plate rheology and cross-polarized optical microscopy.

The third goal is to find out whether liquid crystalline epoxies follow the gelation theory presented by Flory (Flory 1953), which states that the extent of reaction at the gel point is constant regardless of the cure temperature and to examine the conversion dependence of the phase transformations that occur during cure. In this dissertation, Chapter 2 deals with the first goal and Chapter 3 deals with the second and third goals.

CHAPTER 2
SYNTHESIS AND CHARACTERIZATION OF LIQUID CRYSTALLINE EPOXY MONOMERS

2.1 Introduction

Liquid crystalline thermosets (LCTs) are one branch of liquid crystalline materials, which possess the outstanding properties of liquid crystals as well as the high performance properties of thermosets.

Among LCTs, liquid crystalline epoxies (LCEs) have been intensively studied because of their relatively well-known chemistry. However the study of thermal stability and the actual comparison of thermal stability between different phases of same liquid crystalline materials are rare.

Dynamic thermogravimetric analysis (TGA) is a commonly used method to measure and compare the thermal stability of materials. TGA data gives the threshold temperature for the degradation of a material via measurement of the weight remaining during heating at constant heating rates. By comparing the temperatures for a certain weight loss, the relative stability of materials can be compared. (Gavrin 1999)

This chapter deals with the synthesis of DOMS and a novel liquid crystalline thermoset, D2A1 which is obtained from the reaction between DOMS and aniline. Thermal analysis of the synthesized LCEs, DOMS and D2A1, are studied and compared. Also comparison with a non-liquid crystalline conventional epoxy, diglycidyl ether of bisphenol A (DGEBA) is discussed.

2.2 Experimental Section

2.2.1 Synthesis of 4,4'-diglycidyloxy-α-methylstilbene (DOMS)

DOMS synthesis was performed by the method reported in the literature. (Earls et al. 1992, Giamberini et al. 1995a) Elemental analyses were determined at the department of Chemistry at the University of Florida.

Materials. Phenol (99%), chloroacetone (96%), dichloromethane (99.9%), epichlorohydrin, concentrated sulfuric acid, isopropanol (99%) and sodium hydroxide were used as received from Acros without further purification.

Synthesis of 4,4'-dihydroxy-α-methylstilbene (Diol). Phenol (500 g, 5.31 mole), chloroacetone (222.54 mL, 2.65 mole) and dichloromethane (300 mL) were cooled to –10°C with mechanical stirring in a 1-L beaker in a temperature-controlled cold bath. When the solution became clear, sulfuric acid (141.52 mL, 2.65 mole) was added dropwise over 2hours by dropping funnel. After the completion of sulfuric acid addition, the mixture was reacted for additional 2hours with stirring at -10°C. The viscous orange colored product was washed with iced deionized water by vigorous stirring, and when the stirring was stopped the product and water layer were separated. Then the water layer was decanted. Washing was repeated about 30 times until the product became a pink slurry. The product was dissolved in about 700 mL of ethyl alcohol in a 2-L beaker at room temperature and then an amount of distilled water equal to the amount of ethyl alcohol used was added slowly with stirring. After the addition of water, the solution was boiled for 5-6 min and then slowly cooled overnight for recrystallization. The precipitate was filtered and recrystallized repeatedly until the liquid became pH neutral. The pH was checked with pH paper. The white crystalline product was washed with deionized water

and dried overnight in a vacuum oven at 70°C. Elemental analysis (EA) data for theoretical and experimental values are shown in Table 2-1.

Table 2-1. EA results for Diol

	Theoretical value	Experimental value
C (%)	79.646	77.026
H (%)	6.195	6.550
O (%)	14.159	16.424

Synthesis of 4,4'-diglycidyloxy-α-methylstilbene (DOMS). 4,4'-dihydroxy-α-methylstilbene (100g, 0.44mole), epichlorohydrin (346.1mL, 4.425mole), isopropanol (281.6mL, 54wt% of epichlorohydrin used), and distilled water (32.75mL, 8wt% of epichlorohydrin used) were added to a three neck flask and refluxed under argon atmosphere. The epichlorohydrin added were a lot excess to make sure the epichlorohydrin was reacted to the end of 4,4'-dihydroxy-α-methylstilbene molecules. 20% NaOH solution (38.9g, dissolved in 155.6mL of deionized water) was prepared. 1/3 of the NaOH solution was added to the refluxing mixture dropwise and reacted for 1hr. Then stirring was stopped and the mixture was allowed to settle to form two layers. The water layer was then removed. This procedure was repeated two more times with the addition of the rest of NaOH solution. The solution was poured into distilled water and a white solid precipitated out. This solid was filtered and washed with acetonitrile to dissolve out excess epichlorohydrin. The product was filtered and dried in a vacuum oven at 50°C. Elemental analysis data for theoretical and experimental value are shown in Table 2-2.

Epoxy equivalent weight (EEW). The epoxy content of the epoxy resins is expressed as epoxide equivalent weight (EEW) or weight per epoxy equivalent (WPE),

which is defined as the molecular weight per epoxy group.

Table 2-2. EA results for DOMS

	Theoretical value	Experimental value
C (%)	74.648	73.916
H (%)	6.503	6.743
O (%)	18.849	19.341

The epoxy content, in equivalents per 100g, is the reciprocal of EEW multiplied by 100. And the epoxy oxygen percentage (%) is 1600 per EEW, which is 16 times to the epoxy content. A common chemical method for analysis of EEW is titration of the epoxide ring by acid.

In this study, the EEW was measured by the method from the literature. (May 1988) Concentrated aqueous hydrochloric acid (26mL) was added to dimethylformamide (1L) as a hydrochlorination reagent and mixed thoroughly with stirring. A 0.1N sodium hydroxide solution in methanol was used as received from Acros. About 2-4meq of DOMS was weighed and dissolved with stirring in exactly 25mL of the hydrochlorination reagent and allowed to stand for 15 minutes at room temperature. Then the excess acid was titrated with the sodium hydroxide solution by checking with the pH meter. Two blank tests, which had no DOMS samples in hydrochlorination reagent, were performed identically.

The EEW was calculated as follows.

$$EEW = \frac{C}{[N(B-A)]}$$

where A is the volume (mL) of sodium hydroxide solution used to titrate the DOMS, B is the volume (mL) of sodium hydroxide solution used to titrate the blank, C is

the weight (mg) of DOMS, and N is the normality of the sodium hydroxide solution. The resulting EEW of the synthesized DOMS ranged from 177 to 202.

Sample preparation (Formulation). Sulfanilamide (SAA, 99.0 %), purchased from Aldrich Chemical Co., was used without further purification as a crosslinking agent. A weighed amount of DOMS was put into a 60 mL Qorpak® bottle. The sample in the bottle was placed in a convection oven at 170°C to be melted. Once the sample started to melt, the temperature was set to 150°C. After the sample was melted into clear yellow melt, a stoichiometric amount of sulfanilamide was added to the melt as follows,

amount of SAA added = (43.05 / EEW of DOMS) x weight(g) of DOMS used

The mixture was occasionally stirred to dissolve all the sulfanilamide in the melt. After the complete dissolution of sulfanilamide, the mixture was taken from the oven and degassed. The mixture was then poured into an aluminum boat and kept in a freezer to prevent further reaction.

Cross-polarized optical microscopy (POM). The liquid crystalline phases and transition times were determined by cross-polarized optical microscopy. The POM data were obtained by utilizing a Nikon Fluorophot microscope and a Linkham Scientific Instrument HFS91 hot stage controlled by a TMS 91 temperature controller. A small amount of the DOMS formulation was placed between two 12mm round, glass microscope cover slips and heated at a rate of 10°C/minute to 400°C. Samples were observed between cross polarizers.

Differential scanning calorimetry (DSC). To conform the phase changes of DOMS, differential scanning calorimetry (DSC) was performed utilizing a Seiko Instruments SSC5200 DSC220C with an SDM5600H data station.

2.2.2 Synthesis of D2A1

The method used to synthesize D2A1 was adopted and modified from the Carfagna group (Ambrogi et al.1999, Ambrogi et al. 2002).

Materials. Aniline (99.5 %) was obtained from Acros and purified by distillation under reduced pressure because of its high boiling point (184-186°C). Aniline is colorless when freshly distilled, and then darkens on exposure to air and light. Acetic acid (99.0 %) and 1,4-dioxane (99.0%) were used as obtained from Acros without further purification.

Synthesis of D2A1. DOMS (10 g, 0.028 mole) was dissolved in 1,4-dioxane (20mL) in a 250 mL three-neck flask with stirring and heating. When the DOMS was fully dissolved, distilled aniline (1.286 mL, 0.014 mole) was added dropwise. To this solution, 10-15 drops of acetic acid were added. Then the solution was refluxed for 2hr 30min at 120°C and poured into chilled hexane (1 L) to induce precipitation. It was kept in the refrigerator overnight. Precipitates were recovered by filtration and dried in the vacuum oven at room temperature. Elemental analysis data for theoretical and experimental value are shown in Table 2-3.

Cross-polarized optical microscopy (POM). With POM, the LC phase changes were determined as in DOMS.

Curing tests with diamine. A weighed amount of D2A1 was put into a 60mL Qorpak® bottle. The sample in the bottle was placed in a convection oven at 135°C to be melted. Once the sample started to melt, the temperature was set to 110°C. After the sample was completely melted, stoichiometric amounts of trans-1, 4-diaminocyclohexane (DACH), phenylene diamine (PDA), or 2,4-diaminotoluene (DAT) were added to each melt and stirred vigorously to mix thoroughly. The mixture was poured into an aluminum

boat and kept in the freezer to prevent further reaction. All the curing agents were used as purchased from Acros.

Table 2-3. EA results for D2A1

	Theoretical value	Experimental value
C (%)	75.159	73.785
H (%)	6.388	6.879
N (%)	1.751	1.172
O (%)	16.702	18.164

Curing tests with anhydrides. A weighed amount of D2A1 was put into a 60mL Qorpak® bottle. The sample in the bottle was placed in a convection oven at 135°C to be melted. Once the sample started to melt, the temperature was set to 110°C. After the sample was completely melted, stoichiometric amounts of hexahydrophthalic anhydride (HHPA), cis-1,2,3,6-tetrahydrophthalic anhydride (THPA) or phthalic anhydride(PA) were added to each melt. Either 0.3wt% or 0.5wt% of 1-methyl imidazole (99.0%) was added to the HHPA sample bottles as a catalyst and 0.3wt% of 1-methyl imidazole was added to THPA and PA sample bottles as a catalyst. The mixture was vigorously stirred to mix thoroughly. The mixture was then poured into an aluminum boat and kept in a freezer to prevent further reaction. All the curing agents were used as purchased from Acros.

Curing tests with catalytic curing agents. 1-methyl imidazole(99.0%) purchased from Acros was used without further purification as a catalytic curing agent. A weighed amount of D2A1 was put into a 60mL Qorpak® bottle. The sample in the bottle was placed in a convection oven at 135°C to be melted. Once the sample started to melt, the temperature was set to 110°C. After the sample was completely melted, 1.5 wt%, 2.0

wt%, or 2.5 wt% of 1-methyl imidazole was added to each melt. The mixture was vigorously stirred to mix thoroughly. When more than 3.0 wt% of 1-methyl imidazole were tried, the cured sample in the oven turned red. The mixture was then poured into an aluminum boat and kept in a freezer to prevent further reaction.

2.2.3 Thermogravimetric Analysis (TGA)

The thermal stability of DOMS was investigated via thermogravimetric analysis (TGA) performed utilizing a Seiko Instruments SSC 5200 TG/DTA. The samples of formulated DOMS were cured in the convection oven programmed according to the known cure cycle of 4h at 150°C, 1h at 175°C and then 4h at 200°C to induce a liquid crystalline state. For comparison, the sample was cured for 3h at 220°C to induce an isotropic state and also a commercial, non-liquid crystalline epoxy, diglycidyl ether of bisphenol A (DGEBA) from Dow Chemical Company was cured according to the cure cycle of the liquid crystalline DOMS. A small quantity (9-12 mg) of the cured sample or neat resin was put in the TGA pan and the weight loss was observed in the dynamic scan under nitrogen flow over the temperature range of 25°C to 1000°C. The heating rates used to calculate the activation energies for thermal decomposition under nitrogen atmosphere were 3, 10, 13, and 40°C/minute.

Thermogravimetric Analysis (TGA) for D2A1 formulated with 2.0wt % 1-methyl imidazole was also performed.

2.3 Results and Discussion

2.3.1 Synthesis of DOMS

Epoxy resins are characterized as a three-membered ring known as an epoxy, epoxide, or ethoxyline group. The ability of an epoxy ring to react with other substrates

gives versatility to the resins and treatment with a variety of curing agent results in insoluble thermoset polymers (Enc 1986).

Epoxy resins are usually prepared by a base-catalyzed reaction between an epoxide, such as epichlorohydrin and a polyhydroxy compound followed by dehydrohalogenation or by direct epoxidation of olefins with peracids.

Synthesis schemes for the diol and DOMS in this work are shown in Figure 2-1 and Figure 2-2. Figure 2-3 shows the mechanism of diol synthesis presented by the Carfagna group. (Ambrogi et al.1999)

Figure 2-4 shows the reaction between the diol and epichlorohydrin to produce the epoxy. (Gao 1997) Reaction of chloroacetone with phenol and sulfuric acid yields the diol. Then the epoxidation of the diol yields the DOMS monomer. By adding excess epichlorohydrin, an epoxy-terminated monomer can be synthesized.

DOMS, known to be a monotropic liquid crystalline material, which shows liquid crystallinity only when it is cooled from the isotropic state, melts at 131°C. (Carfagna 1994a)

Figure 2-5 shows the DSC heating and cooling thermograph of this work. Upon heating, DOMS melts from a crystalline state into an isotropic state and upon cooling from the isotropic state, it shows a nematic liquid crystalline state, then crystalline state. Liquid crystalline phase change temperatures determined by cross-polarized optical microscopy are shown in Table 2-4.

These data are similar to the results of other groups (Barclay et al. 1992, Earls et al. 1992, Lin et al. 1997). Some differences may exist due to differences in synthesis methods and purities.

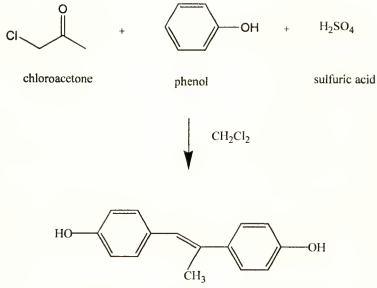

Figure 2-1. Synthesis scheme for Diol

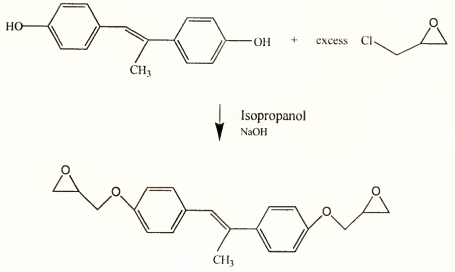

Figure 2-2. Synthesis scheme for DOMS

Compared to enantiotropic LC behavior which has thermodynamic stability within a temperature range between the crystalline melting point and the isotropization point, monotropic LC behavior is metastable for the entire temperature range. In this case, an LC phase is observed when cooled from the isotropic state where crystallization is bypassed by undercooling caused by the kinetically controlled nucleation process (Jing et al. 2002).

In the liquid crystalline state, the epoxy shows a typical Schlieren texture. The common way to get a liquid crystalline crosslinkable monomer is to attach a reactive functional group, such as an epoxide, to the mesogenic structure. However the mesogenic group in the epoxy resin is not sufficient to show liquid crystallinity by itself. Therefore the properties of the curing agent or thermal history during cure play an important role in the formation and maintenance of liquid crystallinity. For example, if DOMS is cured with N-ethylaniline or benzenesulfonamide, liquid crystallinity cannot be obtained.(Liu 1997) If cured with diaminotoluene, a nematic LC phase can be obtained. (Carfagna 1993, Amendola 1996) In this study, a tetrafunctional amine, sulfanilamide (SAA) was used as a curing agent. DOMS is known to be cured in smectic LC phase with SAA. (Sue 1997) Figure 2-6 shows the schematic of the materials used in this study.

As can be seen in this figure, SAA contains two different kinds of amino groups with different reactivities. Normally, there are several reactive groups in the epoxy-curing agent system.

When there is a predominant reactive group whose reactivity is significantly higher than the others, the reaction between the epoxy and other groups can be neglected and the system can be described as a simple autocatalytic model such as in the case of

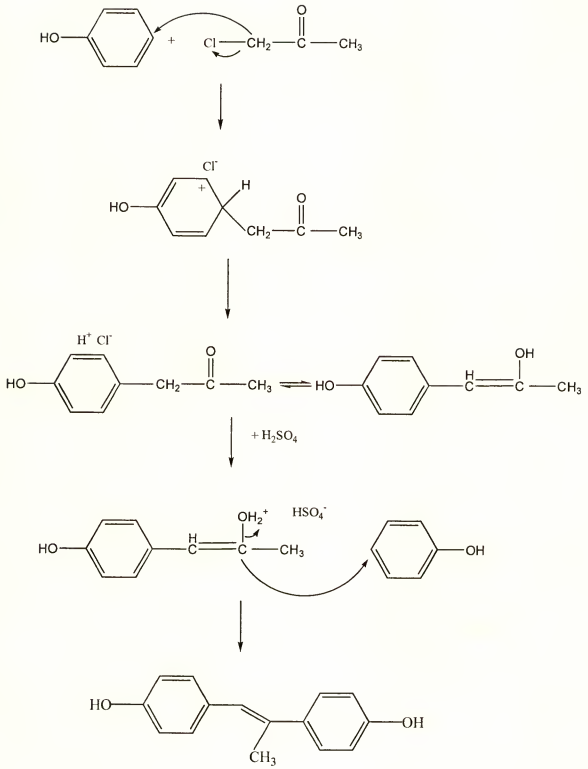

Figure 2-3. Synthesis Mechanism for Diol

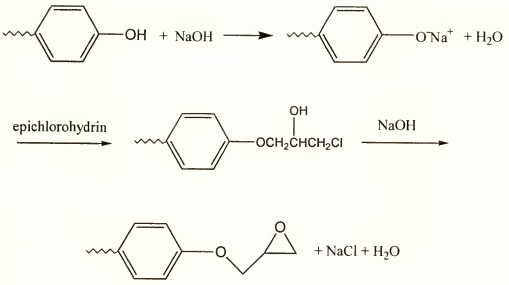

Figure 2-4. Synthesis steps of DOMS from diol and epichlorohydrin

Table 2-4. Transition temperatures of DOMS

Observed transition Temperature (°C)		Comments
On heating	129.5	Crystalline to isotropic
On cooling	109.4	Isotropic to smectic
	72.0	Smectic to crystalline

monofunctional aliphatic and aromatic amines reacting with an epoxy resin without catalyst. However, according to Liu et al. (1997), in the DOMS-SAA system, there are at least five reactive groups such as aromatic primary amine, aromatic secondary amine, primary sulfonamide, secondary sulfonamide, and the nascent hydroxyl formed during curing. When an epoxy group reacts with an amino group with proton donor, an active hydrogen of proton donor weakens the C-O bond in the epoxy ring. The resulting partially positive carbon is attacked by the nitrogen from the amino group and forms a chemical bond such as C-O-C or N-C.

The reactivity is higher for the stronger nucleophilicity of the reactive group. The nucleophilicity of the functional group is characterized by the dissociation constant (K_a) of their conjugated acid and a higher pK_a ($-\log K_a$) means a higher nucleophilicity of the reactive group. The values of pK_a for aromatic primary amine, aromatic secondary amine, primary sulfonamide are 4.6, 5.1 and –3.3 respectively. (Liu et al.1997)

Due to these unequal reactivities, the liquid crystalline network formed with DOMS and SAA occurs step by step (Liu et al.1996).

Figure 2-7 shows the reactions between epoxy and amines or anhydrides, which are most widely used curing agents for epoxy resins (Enc 1986, Mauri et al. 1996, Laza et al. 1998, Park et al. 1998).

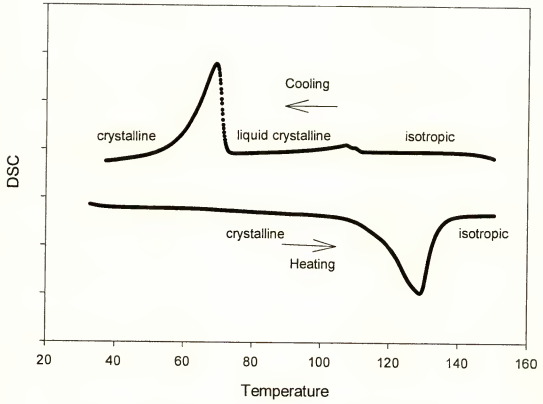

Figure 2-5. DSC thermograph for DOMS (10°C/min, N_2)

DOMS epoxy

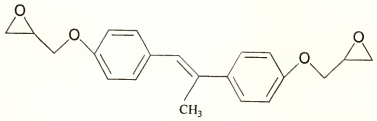

Sulfanilamide

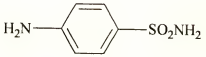

Figure 2-6. Scheme of DOMS and sulfanilamide

Since the sulfone group strongly withdraws the electrons of the nitrogen atom in the amine group, the basicity of the amine is quite low. In fact, because the nitrogen atom on the SAA amide group is negatively charged, the hydrogen atom attached to the nitrogen becomes acidic and acts as a weak acid. Thus, the two reactive groups on SAA have opposite and unequal reactivities of a weak base and a weak acid (Shiota et al. 1997c).

Lin et al. (1997) compared SAA with a difunctional curing agent, with which the curing reaction of the epoxy causes only chain extension. In that case, branching and crosslinking occurs only when the epoxy reacts with the hydroxyl group produced by the epoxy-amine reaction. Since the reactivity of the hydroxyl group is much lower than the reactivity of the amine group, the reaction of the hydroxyl group with epoxy occurs only at temperatures higher than 150°C or in the case of large excess of epoxy amounts. However SAA, a tetrafunctional curing agent causes branching and crosslinking as well as linear chain extension due to the presence of four amine groups. When a rigid-rod epoxy compound is reacted with the curing agent SAA, the formation of an ordered phase during cure is enhanced by using this diamine in which the two amine groups have unequal reactivity. This unequal reactivity leads chain extension to occur prior to branching and eventual crosslinking. The more reactive group of the dual-reactivity curing agent behaves as a chain extension agent while the lower reactive group subsequently completes the crosslinking reaction. It leads to the formation of linear polymer sections, allowing enough time for liquid crystalline organization to occur at the elevated cure temperatures, leading to the formation of a smectic structure, then via cross-linking, locking in the liquid crystalline order.

Curing mechanism with diamine :

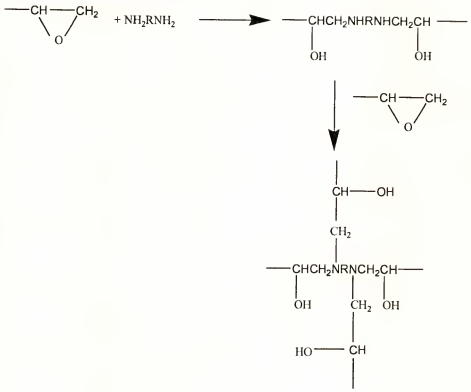

Figure 2-7. Curing mechanism

Curing mechanism with anhydride (Park et al. 1998)

Initiation:

Propagation:

Esterification

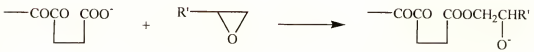

Etherification

Figure 2-7. Curing mechanism (continued)

WAXS patterns (Lin et al. 1997) for DOMS-SAA displays the typical WAXS pattern of a layered structure with two major diffraction peaks, one for intermolecular correlation at $2\theta = 20°$ and the other for the layer spacing at $2\theta = 4.0°$. These results represent that the cured liquid crystalline epoxy have a layered structure of layer thickness of 22.1Å which corresponds to the distance between crosslinks, i.e. the length of DOMS molecules excluding SAA molecules.

2.3.2. Synthesis and Curing of D2A1

Synthesis of D2A1. The synthesis method for D2A1 was adopted and modified from the Carfagna group (Ambrogi et al. 1999, Ambrogi et al. 2002). Figure 2-8 shows the synthesis scheme for D2A1.

The polarized optical microscopy of D2A1 is shown in Figure 2-9. As can be seen in the figure, D2A1 was smectic at room temperature and turned to nematic at 85°C when heated, then turned isotropic at 135°C. When it was cooled from the isotropic liquid, a nematic phase was present at 135°C and turned to smectic at around 80°C again.

The analysis results from the POM data are shown in Table 2-5. This material showed smectic glass texture from the starting room temperature. The DSC scanned from 30°C to 150°C at 10°C/min rate confirmed these transition temperatures.

Curing of D2A1. Optimum performance properties of the epoxy are obtained by cross-linking the epoxy resin into a three-dimensional infusible and insoluble network. The choice of the resin to be treated with a curing agent or hardener depends on curing conditions, processing methods and the desired chemical or physical properties. Primary and secondary amines and anhydrides are the most widely used curing agents for epoxy resins. Normally, the reaction between epoxy and anhydride is so slow that a small

amount of accelerator, such as tertiary amine or imidazole, is added to speed up the cure process as shown in Figure 2-7. It is known that esterification and etherification are the principal curing reactions for this system.

Table 2-5. Analysis results from POM of D2A1

Observed Transition Temperature (°C)	Comments
83	Smectic to Nematic
135	Nematic to Isotropic

When an epoxy resin is cured with an anhydride, the reaction between the tertiary amine and the epoxy group produces zwitterions containing a quaternary nitrogen atom and an alkoxide anion at the initiation step. Then the alkoxide reacts with an anhydride group to produce a monoester, which reacts with an epoxy group to produce the diester.

The etherification reaction is an epoxy homopolymerization which is a competing reaction of the epoxy with an alkoxide anion resulting in an ether linkage. The etherification reaction, which has been known to be slower than the esterification, is responsible for the optimum cured properties (Mauri 1996, Park 1998).

Phenylene diamine(PDA), 2,4-diaminotoluene(DAT) and trans-1,4-diaminocyclohexane (DACH) as diamine type curing agents and hexahydrophthalic anhydride (HHPA), cis-1,2,3,6-tetrahydrophthalic anhydride (THPA) and phthalic anhydride (PA) as anhydride type curing agents were tried. 1-methyl imidazole(MI) was used as a catalyst with the anhydrides and also as a catalytic curing agent. The structures of curing agents are shown in Figure 2-10. Figure 2-11 shows an example of determination of the gelation points determined from parallel plate rheology, which is for D2A1 cured with 2.5wt% 1-methyl imidazole at 80°C.

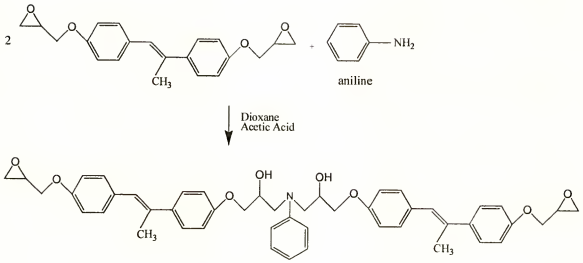

Figure 2-8. Synthesis scheme for D2A1

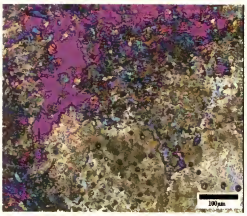

Smectic at 35°C

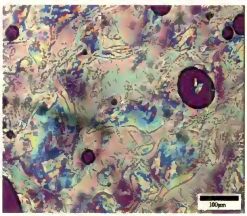

Nematic at 110°C

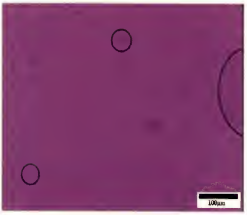

Isotropic at 150°C

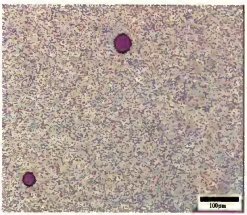

Cooled to smectic

Figure 2-9. Polarized optical microscopy of D2A1

Table 2-6 shows the gelation times for the different curing agents. In D2A1 systems, diamines reacted faster with the epoxy than anhydrides. The gelation times determined with diamines were too short and gelation and vitrification points needed to construct a time-temperature-transformation diagram are not clearly distinguished. The gel times determined with amines were relatively short to decide the order. However when reacted with anhydrides, the clear tendencies related to temperatures and accelerators can be seen.

Higher curing temperature shortened the gel time because molecular mobility becomes higher as temperature increases. And at the same temperatures for anhydrides, higher concentrations of accelerator enhance the gel time due to the increase of reaction rate because more active ionic centers are formed which participates in the subsequent propagation reaction.

The stoichiometric amount of amine needed to cure an epoxy is determined by molecular weight, number of active hydrogens of amine and the EEW of epoxy resin and it is expressed as follows:

amount of amine needed =

((molecular weight of amine)/(number of active hydrogens)) x weight of epoxy used

As with amines, the stoichiometric amount of anhydride needed is as follows:

amount of anhydride needed =

((molecular weight of anhydride)/(number of anhydride groups)) x wt of epoxy used

Since the amines used in this study were tetrafunctional diamines, the number of active hydrogens was 4, and for the case of anhydrides, the number of anhydride groups was 1.

In our study, anhydrides took liquid crystallinity from D2A1 by dilution since 4 times of molar amount of anhydrides were needed for stoichiometric amount than diamines needed. Therefore the catalytic curing agent, 1-methyl imidazole (MI) was used for the construction of TTT diagram.

Table 2-6. Gelation times for various curing agents

Curing agents	Curing temp (°C)	Gel time (min)
PDA	100	7
DAT	100	5
DACH	100	3
THPA-0.3%MI	100	14.5
PA-0.3%MI	90	59.5
HHPA-0.3%MI	100	38
HHPA-0.3%MI	90	48
HHPA-0.3%MI	80	91
HHPA-0.5%MI	90	11
1.5%MI	100	248
2.0%MI	100	85.5
2.5%MI	100	69.5

Although the curing reaction between epoxy and primary or secondary amines occurs via a step growth process, tertiary amines such as imidazoles initiate chain growth polymerization. There have been many research studies about polymerization of epoxy with various imidazoles. (Farkas et al. 1968, Barton et al. 1975, Dearlove et al. 1970, Berger et al. 1985, Ricciardi et al. 1983, Jisova et al. 1987, Chen et al. 1999, Ooi et al. 2000) The cure of epoxy resins with imidazoles exhibits a unique curing behavior in which the starting imidazole can be regenerated during the curing reaction. The

regeneration of imidazole is proven in the literature. (Berger et al. 1985, Ricciardi et al. 1983, Ooi et al. 2000)

2.3.3. Thermal Analysis

There has been research about thermal degradation of liquid crystalline materials by TGA. (Chung 2000, Gavrin 1999, Lu 2000, Pramoda 2000) It is known that generally LCs containing large aromatic repeating units have high thermal stability. A phenylethynyl functionalized highly aromatic LCT did not begin to lose weight until 350°C even in air and 5% weight loss occurred at 507°C in nitrogen at a 10°C/min heating rate (Gavrinet al. 1999). Thermal stability was decreased when the resin was cured with the aliphatic linkage containing curing agent. (Lu et al. 2000) However, research about the effect of different LC phases on the thermal degradation path is rare.

Figure 2-12 shows the TGA scan of the DOMS-SAA system. ISO-DOMS represents the DOMS formulated with SAA and then cured for 3h at 220°C to induce isotropic state and LC-DOMS represents the DOMS formulated with SAA and then cured in the convection oven programmed according to the known cure cycle as follows: DOMS-SAA was cured for 4hours at 150°C, then the oven temperature was raised to 175°C at a ramp rate of 2°C/min and held for 1 hour and again the temperature was raised to 200°C at a ramp rate of 2°C/min and held for 4 hours to induce a liquid crystalline state. The cured DOMS-SAA sample became opaque which is characteristic of liquid crystalline materials. Uncured DOMS is the neat resin without SAA. The TGA scan was performed under a nitrogen atmosphere at a heating rate of 10°C/min. The two curves of the cured DOMS show much higher thermal stability than the uncured neat resin.

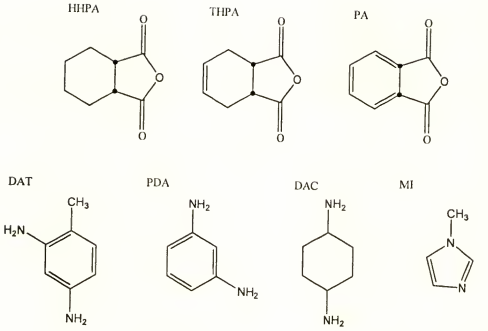

Figure 2-10. Curing agents

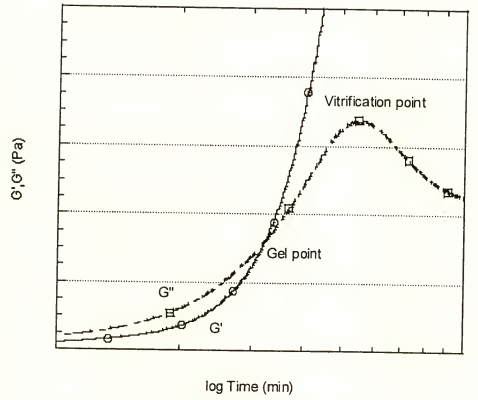

Figure 2-11. Gel point and vitrification point determination

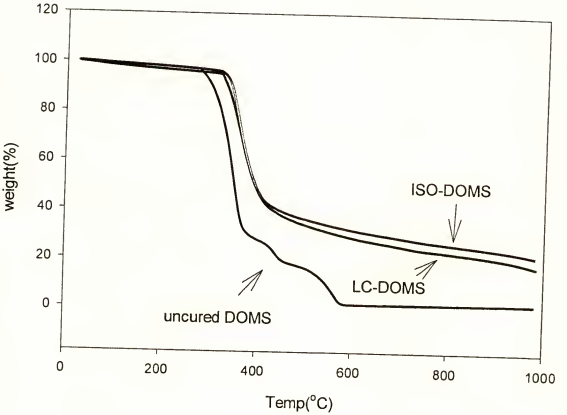

Figure 2-13. TGA scan of DOMS-SAA system
(heating rate 10°C/min, under N_2)

This is due to the fact that crosslinking improves heat resistance because more bonds must be cleaved to exhibit a weight loss or reduction in mechanical properties. However, the thermal stability of the DOMS-SAA system was not affected by the phase differences. This confirms that the important factor which influences thermal stability is the chemical structure and the different phases are not formed by different structures. The TGA curves under nitrogen at 10°C/min rate of DOMS-SAA were compared with a non-liquid crystalline epoxy in Figure 2-13.

A commercial, non-liquid crystalline epoxy monomer, diglycidyl ether of bisphenol A (DGEBA), DER 383 was used. The average EEW used to calculate the amount of SAA to be added was 179.5 from the reported value of 176~183 by DOW. DGEBA was also formulated with SAA and then cured in the convection oven programmed according to the same cure cycle as DOMS; 4h at 150°C, 1h at 175°C and then 4h at 200°C. The chemical structure of DGEBA is shown in Figure 2-13. Comparing the structure of DOMS, shown in Figure 2-6, the structures of DOMS and DGEBA are very similar except the middle part.

As can be seen from the data in Table 2-7, which compares temperatures at 5, 10, 20, 30, 40 and 50% of weight loss for these two epoxies, the difference is not significant which also confirms the importance of structure on thermal stability. The TGA scan for the case of D2A1 was also performed and is shown in Figure 2-15. The LC-D2A1 is D2A1 cured with 2.0 wt% of 1-methyl imidazole for 2 hours at 110°C to be cured in the nematic liquid crystalline phase, iso-D2A1 is D2A1 cured with 2.0wt% of 1-methyl imidazole for 2 hours at 150°C to be cured in isotropic state, and uncured-D2A1 represents the neat resin without the curing agent.

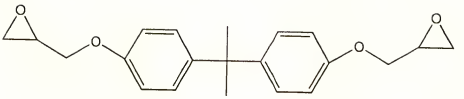

Figure 2-13. Chemical structure of DGEBA

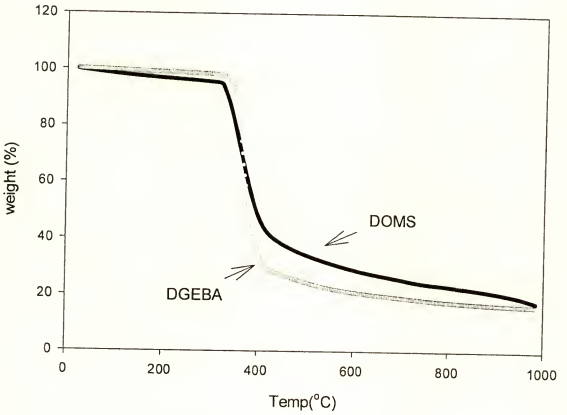

Figure 2-14. TGA scan of DOMS and DGEBA
(heating rate 10°C/min, under N_2)

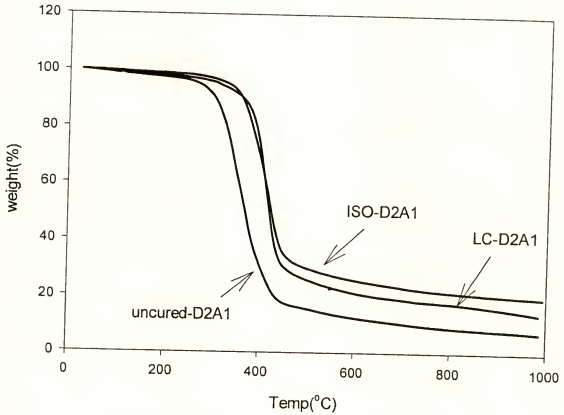

Figure 2-16. TGA scan of D2A1-2.0wt% MI system
(heating rate 10°C/min, under N_2)

Table 2-7. TGA data comparison for DOMS and DGEBA

	Temp for weight loss (°C)					
	5%	10%	20%	30%	40%	50%
DOMS	323	336	351	366	379	397
DGEBA	344	355	362	367	375	383

The TGA scan was performed under nitrogen atmosphere at a heating rate of 10°C/min. As with DOMS, cured D2A1 has higher thermal stability than uncured D2A1 and the phase differences don't affect thermal stability. This result can be analogous to the case of thermal stability of semi-crystalline vs. amorphous polymers. Penco et al. (2000) compared the TGA results of different ratios of multiblock copolymers which showed amorphous or semicrystalline morphologies with different crystallinity. The thermal degradation results were influenced by the characteristics of each component of copolymer rather than by the actual crystallinity itself, i.e., one copolymer started to degrade at 284°C with 63.6% crystallinity and another copolymer started to degrade at 328°C with 19.5% crystallinity because of the difference of composition of each block, which had different thermal degradation temperatures.

When semicrystalline polyester, poly (ethylene terephthalate) (PET) was copolymerized with poly (ethylene nitroterephthalate) (PENT) to produce amorphous polymer, the thermal degradation temperature was lowered. However it could not be explained by crystalline vs. amorphous phase differences because the homopolymer of PET used had a 50°C higher thermal stability than the PENT homopolymer. (Kint 2000) Furthermore, the direct comparison of thermal stability of amorphous poly (ether ether

ketone) (PEEK) and semicrystalline PEEK with 33% crystallinity results revealed no difference in degradation temperature (500°C for both) even though tensile modulus and other physical properties had differences. (Bai et al. 1991) Therefore as was explained, we may conclude that the most important factor which influences thermal stability is the molecular structure and the chemical bonds with which the molecules are connected, rather than the alignment of the molecules.

Activation energies for degradation. Extensive research has been done to investigate the thermal stability or calculate the activation energies for decomposition for polymers using TGA. (Liaw et al. 1994, Dyakonov et al. 1996, Liu et al. 1998, Lee et al. 2000) Activation energies for decomposition (E_d) of DOMS-SAA and D2A1-2.0 wt%MI under nitrogen atmosphere were calculated according to the technique of Flynn-Wall (Flynn 1966) which allows determination of E_d as a function of conversion α by a weight loss process.

The Flynn-Wall method can be expressed as follows,

$$\ln q = C - (E_d/R)(1/T)$$

where E_d is the overall activation energy for weight loss measured at conversion α, q is the heating rate, C is a constant, R is the gas constant and T is the absolute temperature where conversion α is reached at heating rate q.

For thermogravimetric measurements, conversion can be defined as the ratio of actual weight loss to total weight loss corresponding to a given stage of the degradation process as follows,

$$\alpha = (M_0 - M_t) / (M_0 - M_\infty)$$

where M_0 is the initial mass, M_t is the residual mass at time t and M_∞ is the residual mass after completion of weight loss process.

Figure 2-16 represents the Flynn-Wall plots of ln q vs. 1/T for the DOMS-SAA system and Figure 2-17 shows an example of the calculation of the activation energy at α=0.40 for the D2A1-2.0wt% MI system. The calculated activation energies for DOMS-SAA system are plotted in Figure 2-18 and the activation energies are pretty constant which means in this system, the same reaction mechanism is acting on thermal decomposition with a constant activation energy over the examined range. Figure 2-19 shows the same tendency for D2A1-MI system except low conversion range (α<0.15). At low conversion, the volatilization of the unreacted molecules or moisture may influence the decomposition process. (Lee 2000)

Liaw et al. (1994) investigated the thermal decomposition of acrylated diglycidyl ether of bisphenol-S (DGEBS) and DGEBA and calculated the kinetic parameters. They reported E_d as 152.67 ~ 378.19 kJ/mole for DGEBS and 129.38 ~ 202.01 kJ/mole for DGEBA at conversion 5~80%. Lee et al. (Lee 2000) compared the activation energies of DGEBA/4,4'-methylene dianiline system with toughener calculated by different methods and they reported activation energies of 184, 182 and 222 kJ/mole. Recently, Lu et al. (Lu 2000) calculated the activation energies of liquid crystalline epoxy systems. Diglycidyl ether of biphenol cured with methylene dianiline showed higher activation energies (101~207 kJ/mole) than that cured with 4,4'-amino-phenoxy hexane (47~89 kJ/mole). When compared with their results, our systems show activation energies lie in the middle range among other epoxy systems. Since the purpose of TGA study of this system is a direct comparison of thermal degradation path between LC and isotropic

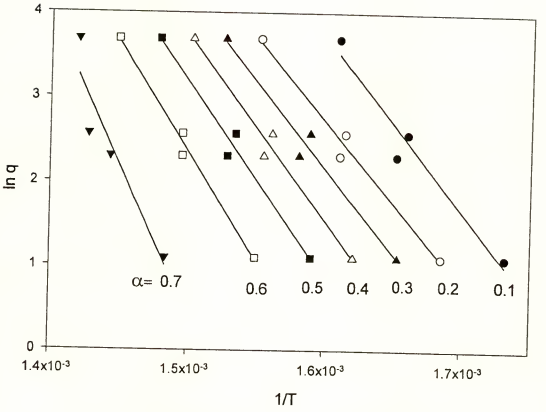

Figure 2-16. Flynn-Wall plot of DOMS-SAA system

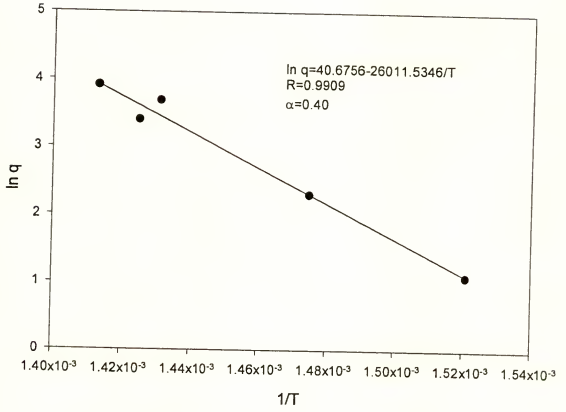

Figure 2-17. Plot of ln q vs. 1/T for α=0.40 for calculation of E_d

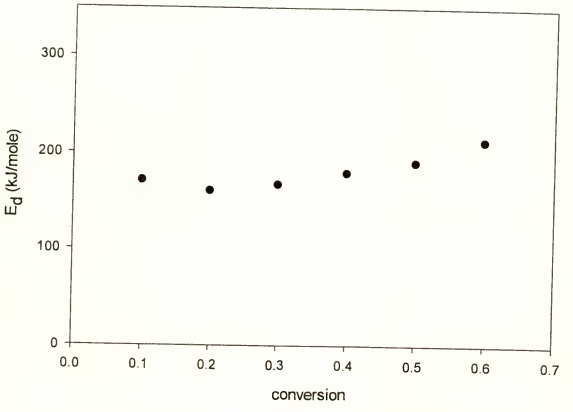

Figure 2-18. Activation Energies for decomposition of DOMS-SAA system

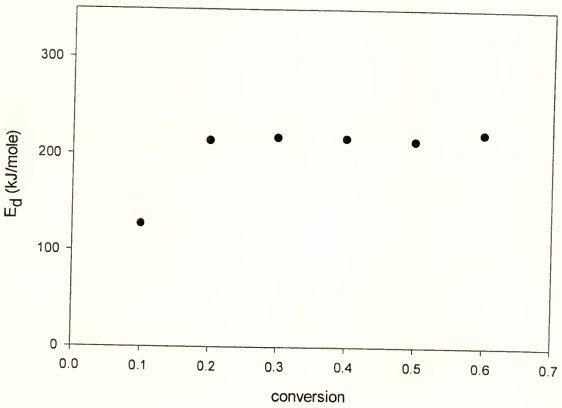

Figure 2-19. Activation Energies for decomposition of D2A1-2.0wt%MI system

There have been many studies to understand kinetics of thermal degradation and many models have been established to investigate the kinetics (Dhar 1986, Horvath et al. 1989, Satava 1971, Vyazovkin and Wight 1999, Wyandt and Flanagan 1992).

Dhar (1986) compared five different methods in determining the kinetic parameters such as the reaction order, the activation energy, and the preexponential factor for nonisothermal kinetics. They showed there were from 10 to 32% errors from model to model. Wyandt and Flanagan (1992) also compared three nonisothermal kinetic techniques and found none of the methods were perfect to understand the kinetics.

Horvath et al. (1989) considered the entropy of activation determined from isothermal TGA as a possible structure-sensitive parameter. They found there are no simple relations between crystallinity and activation energy of decomposition in their clay system, but found the relationship between crystallinity and activation entropy by empirical straight line function of which activation entropy value increases as crystallinity decreases.

In our system, the preexponential factor calculated for D2A1-2.0wt% system in nematic phase at conversion of 0.4 was about 40 as seen in Figure 2-17, and for DOMS-SAA system in smectic phase at the same conversion was about 38. There's no significant difference found for these two systems. This further confirms that in these two LC epoxy systems, phase differences did not influence the mechanism of degradation because the preexponential factor term is closely related to the mechanism and kinetics.

There are arguments between isothermal and dynamic TGA regarding which technique is better to understand kinetics. The rate constants at each temperature are better defined in isothermal TGA, however there might differences in the degradation

mechanism and the final residue at different temperatures. Another problem arises in which the sample must be heated to reach the reaction temperature during which decomposition of sample can occur. Dynamic TGA has advantages such as there are no preheating problems, however it is difficult to explain theoretical kinetic model because of the complicated temperature dependence of the rate constant (Lu 2000). Therefore for more precise understanding complicate kinetics of degradation, both dynamic and isothermal TGA experiments elucidated with several kinds of models would be needed for further study.

2.4 Other Syntheses

2.4.1 Synthesis of Compound II with Hydroquinone Started from Allyl Bromide

The synthesis method of Compound II was adopted from Mallon et al. (Mallon 1993) The synthesis scheme is shown in Figure 2-20. The resulting benzoate showed liquid crystallinity at a temperature range of 150~240°C, however when it was tested by parallel plate rheology, it cured with a brown color.

Synthesis of Compound I. Allyl bromide (10.82mL, 0.125 mole), methyl-4-hydroxy benzoate (16.74g, 0.11 mole) and triethylamine (26mL, 0,1875 mole, 1.5 times of allyl bromide) were dissolved in 150mL of acetone in a 500mL round-bottomed flask. Potassium carbonate (45.6g, 0.33 mole) was added to the flask and the resulting mixture was stirred and refluxed for 24 hours at 75°C. After the reaction was completed the mixture was filtered to remove the salts and the filtrate was evaporated under reduced pressure to yield a light yellow oil. The light yellow oil in the flask was cooled in the ice bath to check if more solid would appear. To this oil, 200mL of 2M KOH (22.45g in 200mL water) solution were added and the resulting mixture was stirred and refluxed for

5 hours. The resulting dark red solution was cooled to room temperature and acidified with HCl to produce a white precipitate which was filtered off, washed with water and recrystallized from 70mL of ethanol. The solid was dried under vacuum. The yield was 81% and the results from the elemental analysis are in Table 2-8.

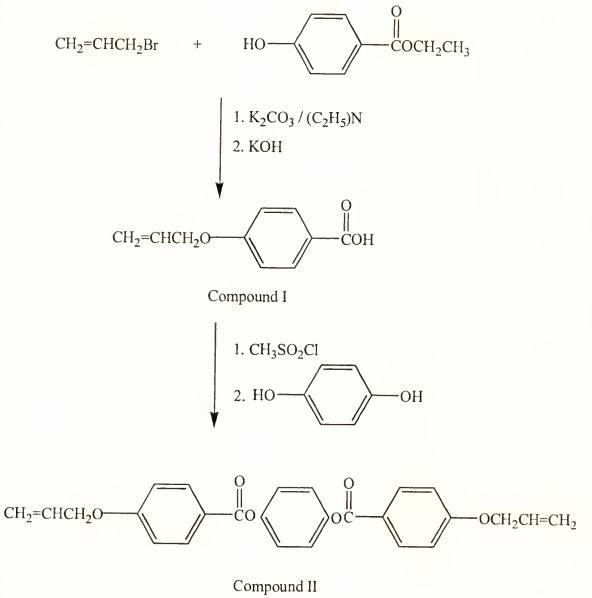

Figure 2-20. Synthesis scheme

Table 2-8. EA results of Compound I

	Theoretical value	Experimental value
C (%)	67.436	66.255
H (%)	5.615	5.681
O (%)	26.949	28.064

Synthesis of Compound II. Synthesized Compound I (9.93 g, 0.05 mole) was placed into 87.6 mL of 1,2-dimethoxyethane (ethylene glycol dimethyl ether) in a 250 mL round-bottomed flask. The mixture was cooled to 0°C with stirring under an Argon atmosphere. To this mixture, triethylamine (15.62 mL, 0.112 mole) and methanesulfonyl chloride (4.34 mL, 0.056 mole) were added slowly and the cooled mixture was stirred for 1.5 hours. Then the dimethoxyethane solution of hydroquinone (3.08g, 0.032 mole in 17.7mL of dimethoxy ethane) was added dropwise to the cooled mixture for 10minutes. The mixture was then warmed to room temperature and stirred for 3 hours. The mixture was filtered to remove a white solid and the filtrate was evaporated under reduced pressure to yield a waxy yellow solid. The solid was recrystallized from ethanol and dried in a vacuum oven. The resulting elemental analysis data are in Table 2-9.

Cross-polarized optical microscopy. The synthesized Compound II melts at 150°C into nematic liquid crystalline phase and at 240°C it became isotropic. The POM results are in Table 2-10.

Table 2.9. EA results of Compound II

	Theoretical value	Experimental value
C (%)	72.548	72.333
H (%)	5.151	5.188
O (%)	22.301	22.479

Table 2-10. Transition temperatures (10°C/min rate)

T_m (°C)	T_{lc} (°C)	T_{iso} (°C)
150	150	240

T_m; melting temperature, T_{lc}; nematic LC transition temperature
T_{iso}; isotropization temperature

2.4.2 Compound III with Methoxy Hydroquinone

Compound I (10.69 g, 0.06 mole) obtained by the same method as described in section 4.1 was placed into 1,2-dimethoxyethane (94.7 mL) in a 500 mL round-bottomed flask. The mixture was stirred and cooled in an ice bath under an Argon atmosphere. Triethyl amine (16.73 mL, 0.12 mole) and methane sulfonyl chloride (4.64 mL, 0.06 mole) were added slowly then the mixture was stirred for 3 hours to induce a light beige colored mud. A dimethoxy ethane solution of methoxyhydroquinone (4.20 g, 0.03 mole in 18.9 mL of dimethoxy ethane) was added dropwise and the mixture was allowed to warm to room temperature and was stirred for another 18 hours. Then the solid was filtered out and the resulting solution was evaporated to induce a solid which was recrystallized from ethanol, washed with water and dried in the vacuum oven.
Via POM, the melting was observed at 140°C but no liquid crystallinity was observed.
Figure 2-21 shows the structure of the product. The EA results are in Table 2-11.

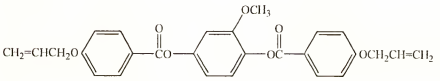

Figure 2-21. Molecular structure of Compound III

Table 2-11. EA results of Compound III

	Theoretical value	Experimental value
C (%)	70.425	70.420
H (%)	5.253	5.377
O (%)	24.322	24.203

2.4.3. Compound IV with Biphenol

Instead of using methoxy hydroquinone as in Section 4.2, p,p'-biphenol (5.59 g, 0.03 mole) was added and the product was recrystallized from N,N-dimethylformamide. The structure is shown in Figure 2-22. EA and POM results are in Table 2-12 and 2-13, respectively. Liquid crystallinity was observed at 170~280°C and when it was tested via parallel plate rheology, it cured to a brown color.

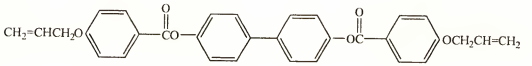

Figure 2-22. Molecular structure of Compound IV

Table 2-12. EA results of Compound IV

	Theoretical value	Experimental value
C (%)	75.876	75.533
H (%)	5.173	5.104
O (%)	18.951	19.363

Table 2-13. Transition temperatures of Compound IV (10°C/min rate)

T_m (°C)	T_{lc} (°C)	T_{iso} (°C)
170	170	280

T_m; melting temperature, T_{lc}; nematic LC transition temperature
T_{iso}; isotropization temperature

2.4.4 Synthesis of Compound VIwith Hydroquinone Started from 8-bromo-1-octene

Synthesis of Compound V. 8-bromo-1-octene (10 g, 0.052 mole), methyl-4-hydroxybenzoate (6.97 g, 0.046 mole) and 18-crown-6 (0.61 g, 0.0023 mole) were dissolved in 63 mL of acetone in a 500 mL round-bottomed flask. Potassium carbonate (19.07 g) was added to the flask and the mixture was stirred and refluxed for 30 hours. The resulting dark orange liquid was filtered to remove salts and the filtrate was evaporated under reduced pressure. To the resulting dark red oil, 84 mL of 2M KOH solution was added and stirred and refluxed for 5 hours. The solution was cooled to room temperature and acidified with HCl to produce a white precipitate which was filtered and washed with water. The solid was recrystallized from ethanol and dried under vacuum at 50°C. The EA results are shown in Table 2-14.

Table 2-14. EA results of Compound V

	Theoretical value	Experimental value
C (%)	72.553	71.340
H (%)	8.118	8.382
O (%)	19.329	20.278

Synthesis of Compound VI. Compound V (4.75 g, 0.019 mole) was suspended in 20mL of benzene with stirring. Oxalyl chloride (4.144 mL, 0.0475 mole) was added very slowly to the mixture under an Argon atmosphere. The mixture was slowly heated and allowed to reflux for 4 hours. Excess oxalyl chloride and benzene were evaporated under reduced pressure. Biphenol (1.65 g, 0.009 mole), ether (24 mL) and triethyl amine (2.5 mL, 0.018 mole) were combined in another flask and allowed to stir in an ice bath for 30 minutes. To this, the synthesized benzoyl chloride was slowly added and stirred for 5 hours to induce a grey muddy solid. Excess ether was evaporated and 40 mL of water

were added and stirred. The solid was isolated by filtration and dried under vacuum at 50°C. The structure is shown in Figure 2-23 and EA results are in Table 2-15. The and when it was tested via parallel plate rheology, it was cured to a brown color.

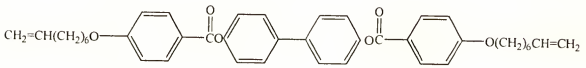

Figure 2-23. Molecular structure of Compound VI

Table 2-15. EA results of Compound VI

	Theoretical value	Experimental value
C (%)	77.991	77.583
H (%)	7.168	7.211
O (%)	14.841	15.206

2.4.5. Synthesis of Compound VII

4,4'-dihydroxybenzophenone (7.49 g, 0.035 mole) and epichlorohydrin (30 mL, 0.28 mole) were dissolved in isopropanol (14 mL) in a 100mL round-bottomed flask. The mixture was heated to 75°C and a 50% aqueous solution of NaOH (3 g, 0.077 mole) was added to the mixture slowly maintaining a gentle reflux. When the NaOH solution was added, the mixture became yellow. Then the reaction mixture was stirred at 78°C for 5 hours. The product crystallized out as a fine light yellow powder. However the product didn't show liquid crystallinity when observed via polarized optical microscope. The reaction scheme is shown in figure 2-24.

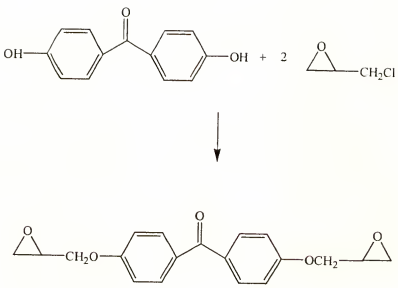

Figure 2-24. Synthesis scheme

2.4.6 Synthesis of Compound VIII with Acetoxy Benzoic Acid

To synthesize the final product shown in figure 2-25, 4-acetoxy benzoic acid (5 g, 0.0278 mole) was suspended in benzene (30 mL) in a 100mL round-bottomed flask with stirring. To this mixture, oxalyl chloride (6.06 mL, 0.0695 mole) was added very slowly and heated to reflux for 3 hours under an Argon atmosphere. The mixture turned cloudy, then cleared. The mixture was cooled and the excess oxalyl chloride and benzene were removed by evaporation. The resulting solution was cooled overnight and recrystallized from acetone. After filtration the solid was dried under vacuum. However the product was corrosive and corroded the door gasket of the vacuum oven. The reaction couldn't be completed.

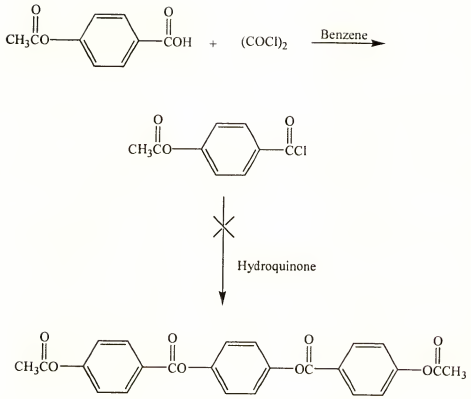

Figure 2-26. Synthesis scheme

2.5 Conclusions

The liquid crystalline epoxy monomer, DOMS and a new liquid crystalline epoxy, D2A1 have been synthesized and characterized. The thermal characterization results showed a monotropic liquid crystalline phase behavior of nematic texture between the temperature range of 109.43°C ~ 72°C on cooling for DOMS. D2A1 showed a smectic LC phase at room temperature and transformed to a nematic phase at 83°C, then cleared at 135°C. The curing tests for D2A1 were performed with diamine type curing agents, such as phenylene diamine, 2,4-diaminotoluene and trans-1,4-diaminocyclohexane, anhydride type curing agents, such as hexahydrophthalic anhydride, cis-1,2,3,6-tetrahydrophthalic anhydride and phthalic anhydride, and catalytic curing agent 1-methyl imidazole. The curing test results revealed that reaction with diamine type curing agents are completed in a short time (< 7 min) at 100°C and anhydride type curing agents destroy liquid crystallinity by dilution in this system. Theses results reveal that gel times can be affected by reactivities of curing agents, concentration of accelerators and curing temperatures. 1-methyl imidazole was chosen for further experiments and characterization.

The results of thermal characterization utilizing TGA confirms that the most important factor influencing the thermal stability is the molecular structure rather than phase differences, even for the LC systems. The activation energies for the decomposition of the DOMS-SAA and the D2A1-MI systems have been calculated by the Flynn-Wall method. By plotting the derivative of conversion vs. the inverse of the absolute temperature at that conversion, activation energies can be obtained from the

slope. The constant activation energies calculated reveal that the same reaction mechanism acts on thermal decomposition for the examined range.

CHAPTER 3
GELATION AND DEVELOPMENT OF LIQUID CRYSTALLINE ORDER DURING ISOTHERMAL CURE OF RIGID ROD EPOXY

3.1. Introduction

As stated in the previous chapters, liquid crystalline thermosets offer characteristic properties for various applications, such as matrices for high performance composites as well as electronic packaging and non-linear optics. As more and more interest is focused on LCTs, understanding changes during cure is needed because for thermosetting materials, useful properties appear only after the curing reaction.

Even though there have been many diagrams constructed to show changes during isothermal cure for thermosets, their scope is limited. They offer useful information for the physical transformations during curing, however they do not present information about phase changes by liquid crystals. On the other hand, experimentally determined liquid crystalline phase transition diagrams do not present the physical transformation information, such as gelation and vitrification. Researchers have also studied the curing kinetics of conventional epoxies and LCTs (Ampudia et al. 1999, Han et al. 1997, Laza et al. 1998, Liu et al. 1998, Micco et al. 1997). Liu et al. (1997) showed the kinetics of DOMS cured with several amines with different functionality. When monofunctional aliphatic and aromatic amines are used as curing agents, the epoxy resin can react with them without catalyst and can be described by a simple kinetic model (i.e. autocatalytic model). However, in the case of a tetrafunctional amine, such as sulfanilamide (SAA), a deviation from the autocatalytic model was seen and a complex kinetic model was

established. There have been relatively few studies undertaken to understand how the crosslinking reaction and liquid crystalline phase structure in liquid crystalline thermosets interact. Jahromi et al. (1995) have shown that gelation occurs at the same conversion as expected for a non-liquid crystalline epoxy, although measurements were made at only a single cure temperature. Lin et al. (1997) have examined the stability of the liquid crystalline phase of DOMS as a function of cure. They showed that the isotropization temperature of the partially cured material increases with increasing cure time, and they presented diagrams illustrating the phase changes that occur during isothermal cure.

In this chapter, there are three primary aims: the first is to construct LCPTTT diagrams which will be of much help to provide guidelines for processing by giving information about liquid crystalline phase transition times as well as physical transformation times during isothermal cure; the second is to test whether liquid crystalline epoxies follow the gelation theory by Flory (1953), which states that the extent of reaction at the gel point is constant regardless of the cure temperature; the third is to examine the conversion dependence of the phase transformations that occur during cure.

3.2 Experimental Section

3.2.1 Materials and Sample Preparation

Synthesis and formulations. Synthesis and formulation methods used were the same as those stated in Chapter 2.

Cross-polarized optical microscopy (POM). To observe structural development of the liquid crystalline epoxy, the DOMS formulation was placed between two 12mm round, glass microscope cover slips and put into a preheated hot stage that was controlled by a temperature controller at the temperatures to be examined and held isothermally.

The samples were cured at 120°C, 130°C, 140°C, 150°C, 160°C or 170°C.

3.2.2 Parallel Plate Rheology

Gelation and vitrification times were determined by utilizing a Paar Physica UDS 200, TC 10 Temperature Controller, and a modified TEK 600 with parallel plate geometry using a 25 mm diameter top plate and a 50 mm diameter bottom plate. The sample chamber and plates were preheated to the curing temperature. Approximately 1g of the DOMS or D2A1 formulation were loaded on the bottom plate and the top plate was lowered to a set gap of 1mm. Then the test was started with a 5% oscillating strain at a 1Hz frequency. The gel time was determined from the crossover point of the storage and loss moduli (tan δ=1) and the vitrification time was determined from the maximum point, which comes after gelation, of the loss moduli curve.

3.2.3. Differential Scanning Calorimetry (DSC)

To investigate the cure behavior of the DOMS-SAA system, differential scanning calorimetry (DSC) was performed utilizing a Seiko Instruments SSC5200 DSC220C with an SDM5600H data station. A small quantity of the DOMS formulation (5-9mg) was weighed into a sealed aluminum pan and placed in an oven to be partially cured for various times. Then dynamic scans were performed within a temperature range of -30˚C to 330˚C at a heating rate of 10˚C/min in a nitrogen atmosphere. The change in enthalpy, ΔH, of the cure exotherm was investigated.

The conversion was calculated as follows.

$$\% \text{ conversion} = (1 - \Delta H_p / \Delta H_o) \times 100$$

where ΔH_p is the cure exotherm for the partially cured sample
and ΔH_o is the cure exotherm for the uncured sample

For the isothermal data, the DOMS-SAA samples were weighed into the sealed aluminum pans and isothermal scans were performed at temperatures between 120°C and 170°C for 120 minutes.

3.3 Results and Discussion

3.3.1 Transition Diagrams

As the curing process goes on, the molecular chains are linked together into a three-dimensional network and the material becomes glassy, crosslinked state from a liquid, low molecular weight state. In analyzing and designing cure processes of thermosetting materials, the time-temperature-transformation (TTT) cure diagrams have been widely used. (Wang and Gillham 1993, Gillham and Enns 1994, Lin et al. 1994, Cadenato et al. 1997, Nunez et al. 1997, Nunez et al. 1998) The basis of TTT diagram construction is a profile of the time to gelation and vitrification at different reaction temperatures. (Gillham and Enns 1994) As stated previously, the useful properties of thermosetting materials appear only after the curing step. The peculiar advantage of the isothermal time-temperature-transformation (TTT) diagram is to graphically illustrate the different regions of a thermosetting system in terms of time and temperature such as liquid, gelled liquid, glass, gelled glass, etc. At isothermal cure, unreacted thermoset typically turns from a liquid into a rubber and then into a glass at cure temperatures below $T_{g\infty}$. And the time to reach this liquid-to-rubber transition is gelation time and it is used to calculate the activation energy for chemical curing reaction. To illustrate liquid crystalline transformation that lacks in conventional TTT diagram, as well as physical transformation, the phase transition times observed via optical microscope are added to construct a new LCPTTT diagram.

DOMS-SAA system. DOMS formulated with SAA was observed by cross-polarized optical microscope with a hot-stage to investigate the liquid crystalline phase changes during isothermal cure. The samples were cured at 120°C, 130°C, 140°C, 150°C, 160°C and 170°C. To measure the gelation and vitrification times, samples were isothermally cured between the parallel plates at 120°C, 130°C, 140°C, 150°C, 160°C and 170°C also. Above this temperature, the samples recovered after the measurements were found to be discolored.

Figure 3-1 shows the liquid crystalline phase-time temperature transformation (LCPTTT) diagram constructed for DOMS-SAA system. Compared to a conventional TTT diagram, this shows liquid crystalline phase transitions as well as gelation and vitrification. The closed circles represent the gelation times when the material converts from a liquid to a gel for the isothermal cure temperature. The open circles represent the vitrification times when a gel converts to a vitrified solid. More studies about the gelation and phase transitions of this system will be discussed in the later part of this chapter. The open triangles represent the times when liquid crystallinity was first observed via optical microscopy and the closed squares are when the whole area is covered by a liquid crystalline phase under the microscope. The area marked A represents the isotropic phase at each temperature and the narrow area marked B represents the isotropic and liquid crystalline biphasic state. The region marked C is the liquid crystalline phase. This diagram shows the well-known transition from isotropic to liquid crystalline phase during cure for the DOMS-SAA system. (Lin et al.1994)

Step-growth polymerization and the packing of rod-like molecules can explain the reaction-induced phase transition during isothermal cure. (Lin et al. 1994, Benicewicz et

al. 1998) As a cure reaction proceeds, DOMS monomers are linked end-to-end. Thus the aspect ratio of growing rod-like molecules increases. At some critical aspect ratio, the formation of an ordered molecular arrangement becomes easier. This happens because the entropy for packing of the rods drives to the more ordered liquid crystalline phase direction. The transition of liquid crystalline texture from isotropic to nematic would have been completed if a curing agent such as diaminotoluene were used. On the other hand when DOMS is cured with SAA in which two amine groups have unequal reactivity, at low conversions, the molecules are linked end to end with singly substituted SAA. As the curing proceeds, the aspect ratio of growing rigid-rod increases and unreacted sulfonamide group will react to form layers between growing molecules. Therefore in the case of SAA, smectic phase is formed from isotropic phase.

During the curing reaction of thermosetting materials, a three-dimensional network is formed as long as one of the components has more than two functional groups. For the DOMS-SAA system it has been shown that the curing reaction begins with linear chain formation, and then branching and crosslinking occurs with an increase in molecular weight. (Lin 1997) The extent of linear chain formation depends on the cure temperature.

The existence of biphasic area in the LCPTTT diagram of DOMS-SAA can be explained as above also. Compared to the LC materials that show liquid crystallinity as monomers, DOMS need time to extend to show liquid crystallinity. Since at higher temperatures, the mobility and reactivity of molecules are higher, the time for molecules to align to show an LC phase would be shorter. Therefore the time for the biphasic area is shorter for higher temperature considering log scale of time in the figure.

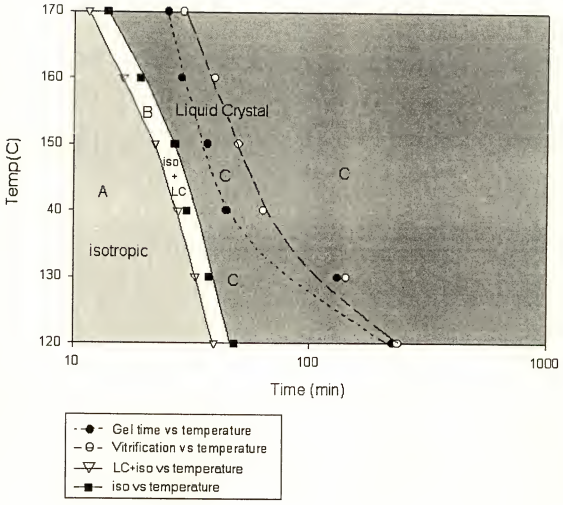

Figure 3-1. LCPTTT diagram of DOMS-SAA system

In the 150°C isothermal scan of the DSC data, a second peak during the reaction appears as seen Figure 3-2. It has been reported (Amendola et al. 1995) that the time of liquid crystalline phase appearance and the maxima of second peaks detected by isothermal DSC might be related. By observing optically via crossed polarizers for the DOMS-diaminotoluene (DAT) system, the reaction mixture is a homogeneous isotropic liquid with a dark image when melted and then a birefringent liquid crystalline phase suddenly appears as the reaction advances. The time for the appearance of the liquid crystalline phases are compared. They conclude that the existence of a second maximum can be explained by the appearance of a liquid crystalline phase during the curing reaction.

When Carfagna et al. (1993) examined the DOMS cured with a certain tetrafunctional amine system there was no second peak found in isothermal DSC data since the system was isotropic when cured. Also the fact that traditional epoxy resins that do not develop ordered structures upon curing, usually show a single exotherm peak during crosslinking has been noted. (Carfagna 1994) Table 3-1 compares these data for our results for the DOMS-SAA system. Due to the use of different instruments, these data don't give us same numbers, but the same trend appears and we can also conclude that the second peak is related to the appearance of liquid crystalline phase formation for DOMS-SAA system.

D2A1-MI system. Figure 3-3 to Figure 3-5 are the TTT diagrams for D2A1 formulated with 1.5wt% MI, 2.0wt% MI and 2.5wt% MI respectively. The open circles represent gelation times when the material converts from a liquid to a gel for the

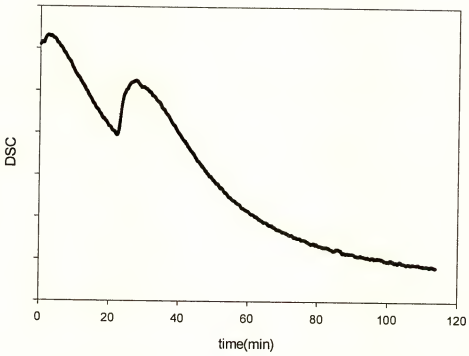

Figure 3-2. Isothermal scan diagram of DSC at 150°C

Table 3-1. Times of liquid crystalline phase appearance by POM(t_{lc}) and second peak maximum of DSC (t_{peak})

T(°C)	t_{lc}(min)	t_{peak}(min)
120	48.03	56.41
130	37.52	45.58
140	30.05	40.91
150	26.70	27.58
160	19.00	23.58
170	14.93	19.75

isothermal cure temperature. The closed triangles represent the vitrification times when a gel converts to a vitrified solid. Especially for the D2A1-2.0wt% MI system, liquid crystalline phases are seen in Figure 3-4. In the D2A1-MI system, the liquid crystalline phases did not change during cure, and exhibited the same liquid crystalline phase as the monomer. In the examined temperature range, we can see the typical S-shaped vitrification curve from D2A1-MI system. The S-shaped curve between T_{go} and $T_{g\infty}$ is due to the fact that as temperature increases the reaction rate also increases. (Sperling 1992) At lower temperatures, the viscosity effect is more predominant than reaction rate constant. Therefore higher viscosity at lower temperatures shortened vitrification time in D2A1-MI system.

According to the theoretical analysis of Fox and Flory (Sperling 1992), the general relationship between T_g and molecular weight M can be expressed as,

$$T_g = T_{g,\infty} - \frac{K}{(\alpha_R - \alpha_G)M}$$

where $T_{g,\infty}$ is the glass transition temperature at infinite molecular weight, α_R and α_G are volume expansion coefficients in the rubbery and glassy states, respectively,

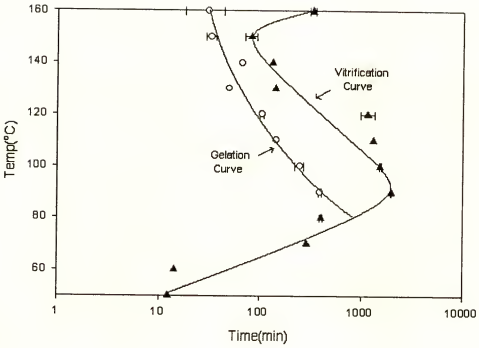

Figure 3-3. TTT diagram of D2A1-1.5wt%MI system

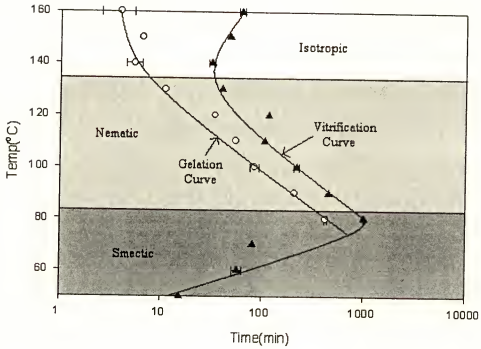

Figure 3-4. LCPTTT diagram of D2A1-2.0wt%MI system

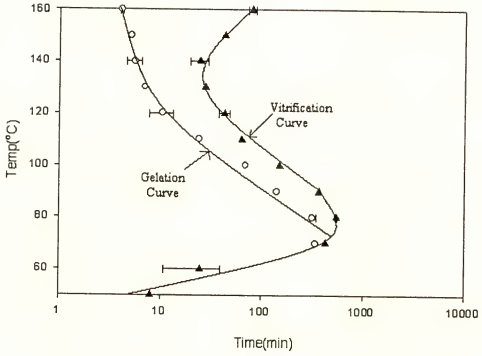

Figure 3-5. TTT diagram of D2A1-2.5wt%MI system

and K is a constant depending on the polymer. Therefore as molecular weight increases, T_g also increases. At higher temperatures in TTT diagram, due to the reaction rate constant, the time to vitrification is shortened. However the time for vitrification starts to increase again, because of the decreasing concentration of reactants needed to be a "critical" molecular weight to show that T_g.

Comparing these diagrams, the more catalytic curing agent added, the shorter the gelation and vitrification times. This is due to the fact that as the concentration of curing agent increases, the reaction rate also increases because more active ionic centers are formed which participate in the subsequent propagation reactions. Chen et al. (Chen 1999) showed that as the concentration of 2-ethyl-4-methyl imidazole increased, the reaction rate of epoxy resin increased. Ooi et al. (Ooi 2000) also presented the cure of DGEBA with 1-MI via DSC at various concentrations, where the peaks shifted to lower temperatures due to an enhanced reaction rate with increasing imidazole concentration.

3.3.2. Gel Points vs. Conversion

The time when the system loses fluidity, i.e. goes from viscous liquid to elastic gel, and the weight average molecular weight becomes infinite, it is called the gel time. The prediction of gel point conversion is especially important in the production of thermosetting materials because beyond this point thermosets cannot be molded or processed.

To predict the extent of reaction at the gel point, Flory and Stockmayer used a statistical approach by calculating when the weight average molecular weight becomes infinite. (Flory 1953, Stockmayer 1951) In this approach, there are two main assumptions, which are (1) the reactivity of all functional groups of a certain kind is the

same and is independent of molecular size and (2) there are no intramolecular connections.

Applying their theory and statistical approach, and assuming a stoichiometric amount is used, the extent of reaction at gel point is expressed as (Cadenato 1997),

$$\alpha_g = \left[\frac{1}{(f-1)(g-1)}\right]^{\frac{1}{2}}$$

where f and g are the functionalities of components used. In our case DOMS is a difunctional epoxy (f =2) and SAA is tetrafunctional amine (g = 4), which results in the value for α_g of 0.577.

Figure 3-6 is the cure exotherm peak scan from DSC at a 10°C/min rate of an uncured sample of DOMS formulated with SAA and placed in a sealed DSC pan and scanned without curing in the oven. The partially cured sample in Figure 3-6 is DOMS formulated with SAA, placed in a sealed pan and partially cured for 20 min at 140°C, then scanned by DSC at 10°C/min rate. As cure proceeds the exotherm peaks got smaller and smoother.

Figure 3-7 shows the conversion at the gel point as a function of cure temperature. This data was obtained by converting the time axis of LCPTTT diagram for the DOMS-SAA system in Figure 3-1 to conversion using differential scanning calorimetry to determine conversion versus time at each temperature. Most notably, Figure 3-7 shows that the isoconversion theory of gelation holds for this system. This is true even though DOMS-SAA experiences different amounts of cure in liquid crystalline phases at different cure temperature. For example, at the cure temperature of 120°C, DOMS experiences liquid crystalline phase for about 64% of conversion until it becomes gel, and

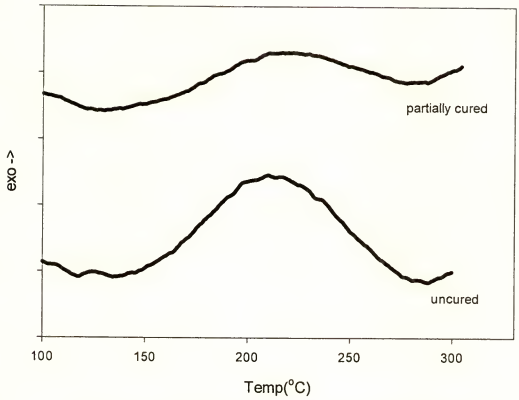

Figure 3-6. Cure exotherm of uncured and partially cured sample

at 160°C it experiences liquid crystalline phase for roughly about 15% of conversion to be gelled i.e. at 120°C cure in the isotropic phase occurs at up to a conversion of 25.17% and at 160°C cure in the isotropic phase occurs up to a conversion of 58.63% even though at both temperatures, gelation occurs at about 70% conversion. Therefore at 120°C considerably more reaction in the liquid crystalline phase occurs before it reaches gelation.

Therefore, even though the amount of reaction that occurs in the liquid crystalline phase is different at different cure temperatures, the isoconversion theory of gelation fits quite well. Thus the gelation is independent of liquid crystalline phases as well as cure temperature.

The experimental average value of the conversion at the gel point is 0.677. The experimental value is slightly higher than the calculated theoretical value of 0.577, and the difference is due to the failure of the assumptions of this theory. In reality, there may be reactivity differences between the same types of functional groups and intramolecular connections are possible. Therefore to reach the critical point, the reaction must go further since some linkages are wasted by intramolecular ring formation. (Flory 1953) Also Stockmayer (1951) stated that although the first of the assumptions can be realized in many practical cases, the second is never correct and possibly causes considerable error in calculations for systems close to the gel point. The conversion at gel point for DGEBA cured with an aromatic amine adduct is known to be 0.62 ± 0.03 (Cadenato et al. 1997), and for DGEBA cured with 1,2-diamine cyclohexane to be 0.61 ± 0.03 (Nunez et al. 1997).

Under the kinetically controlled conditions, the reaction rate can be expressed by an Arrhenius rate expression as follows, (Cadenato et al.1997, Nunez et al. 1997)

$$\frac{d\alpha}{dt} = A\exp\left(-\frac{E}{RT}\right)f(\alpha)$$

where α is the conversion, A is a constant factor, E is the activation energy, T is the isothermal cure temperature and f(α) is the conversion-dependent function, independent of the cure temperature. By integrating from α=0 to α= α_g, the equation becomes,

$$\ln t = \frac{E}{RT} + \left[\ln\left(\int_0^{\alpha_g}\frac{d\alpha}{f(\alpha)}\right) - \ln A\right]$$

Since the terms in the last part of right side of equation are constant for a fixed conversion, the equation becomes,

$$\ln t = C + \left(\frac{E}{RT}\right)$$

By applying the above equation to a series of isothermal experiments for a constant conversion, the activation energy E and the constant C can be determined from the slope and the intercept of the linear relationship between ln t vs. 1/T. This equation can also be used with different degrees of conversion to see if the activation energy changes according to the degree of conversion or how the reaction develops.

Table 3-2 shows the times and conversions at the gel point. As is shown in Figure 3-8, from the Arrhenius plot of ln t vs. 1/T, we obtained an activation energy E=68.4kJ/mol. This is comparable number to the systems of diglycidyl ether of bisphenol A cured with different amines.(Cadenato et al.1997, Laza et al. 1998) Laza et al. (1998) calculated the activation energy of DGEBA cured with triethylenetetramine from the gel time method as 53~71 kJ/mol and Cadenato et al. (Cadenato 1997) calculated for

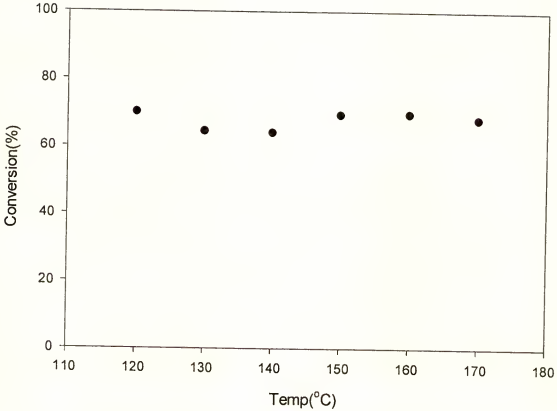

Figure 3-7. Conversion at gelation for DOMS-SAA system

DGEBA cured with aromatic amine adduct HY830 as 47.2~52.9 kJ/mol. The similarity of the activation energy for DOMS/SAA with non-liquid crystalline epoxies further confirms that gelation is unaffected by the liquid crystalline phase.

Table 3-2. gel times and conversion at gel point

T(°C)	t_{gel}(min)	α (%)
120	225.5	70.16
130	131.5	64.56
140	44.5	64.14
150	37.0	69.44
160	28.5	69.71
170	22.0	68.15

3.3.3. Phase Transition vs. Conversion

Figure 3-9 is the plot of phase transition temperature vs. conversion. Closed circles are liquid crystalline transition times and open circles represent the gel times. Table 3-3 shows times of liquid crystalline phase appearance (t_{lc}) and conversion at phase transition. In contrast to gelation, the phase transitions do not show isoconversion behavior. Instead, the conversion at the point where isotropic phase changes to a liquid crystalline phase tends to increase with temperature.

This is due to the fact that the critical length of the molecules needed for the liquid crystallinity increases with temperature. Figure 3-10 is an idealized plot that explains this phenomenon. The straight line shows the increase of isotropization temperature with increasing cure time or molecular length (i.e. conversion).

We note that Fukuda et al. have modeled this increase for thermotropic semiflexible polymers. (Fukuda 1995) They compared and discussed the chain length dependence of the nematic-isotropic transition behavior of semiflexible polymers in the bulk via three

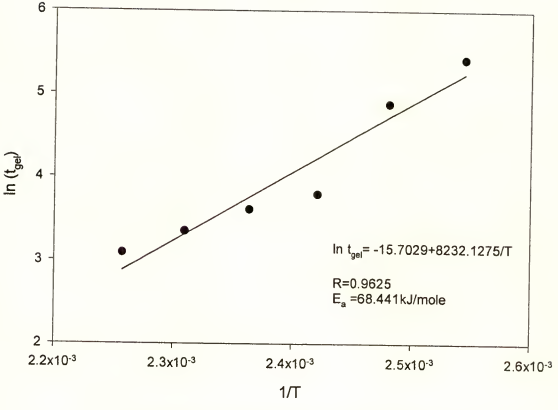

Figure 3-8. Arrhenius plot of ln (t_{gel}) vs. 1/T

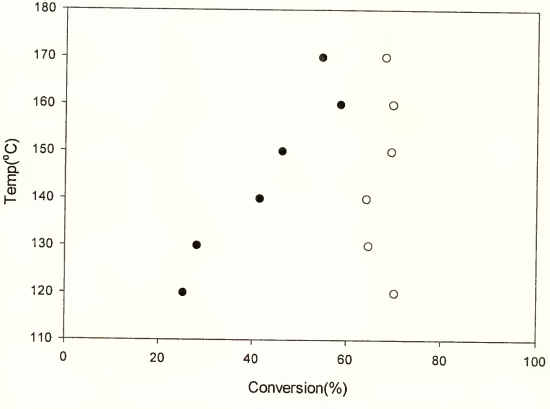

Figure 3-9. Plot of phase transition temperature and gel points vs. conversion

Table 3-3. Times of liquid crystalline phase appearance (t_{lc}) and conversion at phase transition (α_{lc})

T(°C)	t_{lc}(min)	α_{lc}(%)
120	48.03	25.17
130	37.52	28.10
140	30.05	41.49
150	26.70	46.27
160	19.00	58.63
170	14.93	54.73

typical models of orientation dependent interactions such as the Onsager-Kimura type mean field model (Onsager 1949), the lattice version of Onsager model and the Maier-Saupe type soft interaction model (Maier 1958) and two polymer models such as the wormlike chain and the freely jointed chain. They concluded the universality of the isotropization temperature vs. chain length relation scaled appropriately.

It has been observed experimentally by Lin et al. (1997). They cured DOMS with SAA and with a difunctional amine, the aniline adduct of DOMS at one curing temperature of 120°C and developed an isotropization temperature vs. curing time plot. Mormann et al. (1996) also showed the increase of clearing temperature (nematic-to-isotropic phase transition) with increasing conversion for two dicyanates LCT, 4-cyanatophenyl 4-cyanatobenzoate and 4,4'-dicyanatobiphenyl.

As in Figure 3-10, if DOMS is cured at temperature A, it will start to show liquid crystallinity at point X where the straight line and the cure temperature line cross. If the cure temperature increases to B, DOMS needs more time to show liquid crystallinity(X'). Therefore the molecular length needs to be longer; i.e. conversion needs to be higher. Our results which show the increase in isotropic-to-smectic phase transition time as the cure

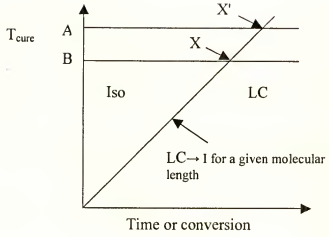

Figure 3-10. Idealized plot for cure temperature vs. time or conversion

By using DSC and optical microscope, they showed that the conversion at the phase change from α=0.41 to α=0.47 as the cure temperature increases from 150°C to 170°C. This suggests that the increase in transformation time with increasing cure temperature is a general phenomenon related to the mechanism of epoxy cure and is independent of the type of liquid crystalline phase that forms. However, Shiota et al. (Shiota 1997b) stated 1, 4-benzenedicarboxylic acid bis(4-cyanatomethylphenyl) ester LCT to show isoconversion behavior for the isotropic-to-nematic transition. In this case the authors attribute the formation of the nematic phase to oligomers with a very high glass transition. Thus the difference between the dicyanate and epoxy systems may be attributed to the mesogenic potential of the monomers and/or oligomers that form early in the reaction.

3.4. Conclusions

The LCPTTT diagram for DOMS-SAA system was constructed by combining data obtained from parallel plate rheology and observed via POM. The TTT diagrams constructed with D2A1-MI system showed typical s-shaped vitrification curve and the amount of curing agents influenced the gelation and vitrification times.

By curing the liquid crystalline epoxy, 4,4'-diglycidyloxy-α-methylstilbene, with the curing agent, sulfanilamide, the isoconversion theory of gelation was confirmed, i.e., the conversion at gelation was uniform regardless of liquid crystalline phase as well as cure temperature. This result indicates that the actual network formed by these molecules is unaffected by any long-range order that may be present, and is only controlled by the functionality of the individual molecules. We note that this study does not address the issue of whether the reaction actually occurs at a faster rate in the liquid crystalline phase,

but rather that gelation occurs in the same manner as non-liquid crystalline epoxies with respect to the conversion dependence and the structure of the resulting network. However, the conversion at the liquid crystalline phase transition points increased with increasing temperature. This phenomenon is due to the increase in isotropization temperature with increasing chain length (i.e. cure time).

CHAPTER 4
CONCLUSIONS AND FUTURE WORK

This dissertation consists of three main goals. One is to synthesize and characterize the liquid crystalline epoxy monomers. The second is to construct transition diagrams, liquid crystalline phase-time-temperature-physical transformation (LCPTTT) diagrams, which will provide us not only physical transformations but also informations about liquid crystalline phase transitions. The third is to examine whether the gelation of liquid crystals also follows iso-conversion theory of Flory (1953) and the conversion dependence of phase transformations occurring during the isothermal cure.

The synthesized monomers, 4,4'-diglycidyloxy-α-methylstilbene (DOMS) melts at 129.5°C and shows a monotropic nematic mesophases upon cooling from 109.4 to 72°C. D2A1 was prepared by the reaction between stoichiometric ratio of DOMS and aniline. D2A1 shows very viscous smectic texture when observed via cross-polarized optical microscopy even at room temperature and upon heating, at 83°C changes to nematic phase and then turns into isotropic at 135°C. The monomers are characterized via cross-polarized optical microscopy, DSC and TGA. Curing of DOMS was performed with tetrafunctional amine, sulfanilamide (SAA) which has two different kinds of amino groups of different reactivities, and the cured DOMS-SAA system shows smectic liquid crystalline phase. Curing tests with D2A1 was performed with various crosslinking agents. Diamine type crosslinking agents such as trans-1, 4-diaminocyclohexane, phenylene diamine, 2,4-diaminotoluene were tried and anhydride type crosslinking

agents such as hexahydrophthalic anhydride, cis-1, 2,3,6-tetrahydrophthalic anhydride and phthalic anhydride were tried with 0.3wt% or 0.5wt% of 1-methyl imidazole as initiator. The curing test results reveal that reaction with diamine type curing agents are cured in short time (< 7 min) at 100°C and anhydride type curing agents take liquid crystallinity by dilution for this system. The catalytic curing agent, 1-methyl imidazole (MI) was tried for curing of D2A1. At the curing temperature of 100°C when 1.5wt% of 1-methyl imidazole was used, D2A1-MI gelled at 248 minutes. At that same cure temperature, D2A1 with 2.0 wt% MI gelled at 85.5 minutes and with 2.5 wt% MI gelled at 69.5 minutes.

Another syntheses to get optimum liquid crystalline thermosets have been also tried. Epoxy benzoate obtained by the reaction of allyl bromide and methyl-4-hydroxy benzoate, then reacted with hydroquinone melts into nematic phase at 150°C and clears at 240°C when observed by cross-polarized optical microscopy. However when tested via parallel plate rheology, it was cured brown color. Benzoate obtained by the reaction of allyl bromide and methyl-4-hydroxy benzoate, and then reacted with methoxy hydroquinone melts at 140°C but doesn't show liquid crystallinity. Benzoate obtained by the reaction of allyl bromide and methyl-4-hydroxy benzoate, then reacted with p, p'-biphenol melts into nematic liquid crystalline phase at 170°C and clears at 280°C. However when tested via parallel plate rheology, it was cured brown color also. The diepoxide obtained by the reaction of 4,4'-dihydroxybenzophenone and epichlorohydrin doesn't show liquid crystallinity.

The thermal stability was tested with dynamic TGA. The comparison between thermal degradation paths of cured and uncured epoxy reveals clear differences with

much higher thermal stability of cured one. However there were no significant differences in thermal stability between isotropic phase and liquid crystalline phase of the same epoxy. This result applied to both DOMS-SAA system and D2A1-2.0wt% MI system. Therefore the dynamic TGA data of DOMS-SAA system was compared with that of commercial, isotropic, non-liquid crystalline epoxy monomer, diglycidyl ether of bisphenol A (DGEBA) cured with SAA, according to the same cure cycle used to get liquid crystallinity of DOMS-SAA. The chemical structure of DGEBA is similar to DOMS except the middle part, where DOMS has double bond in it and DGEBA doesn't.

The thermal degradation path reveals somewhat differences with higher thermal stability of DOMS-SAA system. Since there was no significant differences observed by comparison between isotropic and liquid crystalline phase state of the same epoxy, the most important factor which influences on the thermal stability is the molecular structure itself rather than liquid crystalline phases. The activation energies for decomposition calculated for D2A1-2.0wt% MI system via Flynn-Wall method by plotting ln heating rate vs. 1/T graph indicates that the same reaction mechanism acts on thermal decomposition over the entire range for this system. However the complex kinetics of degradation cannot be explained with this simple experiment, for more precise understanding the complicate kinetics of degradation, both dynamic and isothermal TGA experiments elucidated with several kinds of models would be needed.

The transition diagrams were constructed for both systems. The gelation times and vitrification times are determined via parallel plate rheology and liquid crystalline phases are determined from cross-polarized optical microscopy. The DOMS-SAA system was isothermally cured at temperatures of 120°C, 130°C, 140°C, 150°C, 160°C and

170°C. The D2A1-MI system was isothermally cured at the temperatures between 40~160°C with the temperature increment of 10°C. The time-temperature-transformation diagrams for D2A1 cured with 1.5 wt%, 2.0 wt%, and 2.5 wt% MI showed typical s-shaped time-temperature-transformation diagrams. As the amount of methyl imidazole were increased, the gel times and vitrification times were shortened. This is due to the fact that as the concentration of curing agent increases, the reaction rate also increases because more active ionic centers are formed which participates in the subsequent propagation reactions.

The liquid crystalline phase-time-temperature-physical transformation (LCPTTT) diagrams were constructed for DOMS-SAA system and D2A1-2.0 wt% MI system. Compared to DOMS-SAA system, the liquid crystalline phases of D2A1-MI system doesn't show significant changes as the reaction proceeds. However, DOMS-SAA system melts into isotropic phase first, and then the liquid crystalline phases emerge at different times at different temperatures. The appearance of smectic liquid crystalline phase from isotropic state of DOMS-SAA system is due to the unequal reactivity of curing agent, SAA. This unequal reactivity leads chain extension to occur prior to branching and eventual crosslinking. The more reactive group of the dual-reactivity curing agent behaves as a chain extension agent while the lower reactive group subsequently completes the crosslinking reaction. It leads to the formation of linear polymer sections, allowing enough time for liquid crystalline organization to occur at the elevated cure temperatures, leading to the formation of smectic structure, then via cross-linking, locking in the liquid crystalline order.

The final goal deals with the examination of applicability of Flory's gelation theory to the liquid crystalline materials and the conversion dependence of phase transformation during isothermal cure. By comparing the cure exotherm, which were determined from dynamic DSC scan for the partially cured sample to the uncured sample, %conversion data were obtained. The results reveal that even though the amount of reaction that occurs in the liquid crystalline phase is different at different cure temperatures, the isoconversion theory of gelation fits quite well. Thus the gelation is independent of liquid crystalline phases as well as cure temperature. The actual average value of the conversion at the gel point is 0.677, which is slightly higher than the calculated theoretical value of 0.577 due to the failure of the assumptions of this theory, i.e., there might be reactivity differences between the same types of functional groups and intramolecular connections are possible. And by plotting the Arrhenius plot of ln (t_{gel}) vs. 1/T, the activation energy determined was 68.4kJ/mol, which is comparable number to the systems of diglycidyl ether of bisphenol A cured with different amines. The similarity of the activation energy for DOMS/SAA with non-liquid crystalline epoxies further confirms that gelation is unaffected by the liquid crystalline phase.

When the conversion dependence of phase transformations occurring during the isothermal cure was also examined, it was found that the phase transitions do not show isoconversion behavior in contrast to gelation. Instead, the conversion where phase changes from isotropic to a liquid crystalline phase tends to increase with temperature due to the fact that the critical length of the molecules needed for the liquid crystallinity increases with temperature.

This study is an initial work to examine the thermal stability by comparing different phase states of the same liquid crystalline material and similar structured non-liquid crystalline material. This study has shown that the important factor that influences on the thermal stability is rather the molecular structure itself than the liquid crystalline phases even though it is more ordered at liquid crystalline state.

This work has also shown that the new LCPTTT diagrams which are useful in illustrating not only physical transformations but also the liquid crystalline transitions occurring during the isothermal cure process. As expected for the catalytic curing system, the systems with more catalytic curing agent gels and vitrifies in shorter time. And for the case when the system melts into isotropic state first, the liquid crystalline phases emerge at different times at different temperatures.

Finally, it was found that the isoconversion theory also applies to gelation of liquid crystalline thermoset systems as in conventional thermoset systems. This result indicates that the actual network formed by these molecules is unaffected by any long-range order that may be present, and is only controlled by the functionality of the individual molecules. This study does not address the issue of whether the reaction actually occurs at a faster rate in the liquid crystalline phase, but rather that gelation occurs in the same manner as non-liquid crystalline epoxies with respect to the conversion dependence and the structure of the resulting network. However the conversion where phase changes from isotropic to a liquid crystalline phase tends to increase with temperature rather than showing isoconversion.

There are still many questions remaining unanswered. In this study, the comparison of thermal degradation paths between isotropic DOMS-SAA, smectic

DOMS-SAA and non-LC DGEBA-SAA has been conducted only quantitatively. More specific investigations regarding morphology analysis are needed. Furthermore, if oriented LCT systems are included in the study, it will be more valuable. As is well known, LCT molecules can be oriented by the influence of mechanical, electric or magnetic fields and oriented LCTs shows higher mechanical properties. However the thermal stability tests of the oriented LCTs are rare. Therefore the investigations about the oriented LC, un-oriented LC and isotropic systems together will be very interesting.

Another interesting scientific aspect would be determining the influence of stoichiometry of curing agent on the LCPTTT diagrams. Since we know that the unequal reactivity of SAA influences on the smectic phase formation of DOMS, when off-stoichiometric amounts of SAA are used to cure, there might be effects on liquid crystalline phase transition times and/or gelation and vitrification. And those results will be helpful to understand the curing mechanisms and kinetics of DOMS-SAA system. Also another catalytic curing agents can be tried for D2A1 system and for the constructions of LCPTTT diagrams for further investigation of this newly synthesized D2A1 monomer.

LIST OF REFERENCES

Ambrogi, V., Giamberini, M., and Carfagna, C., Discussion of synthesis in 1999

Ambrogi, V., Carfagna, C., Giamberini, M., Amendola, E., and Douglas, E., *J. Adhesion Sci. Technol.,* **16,** 15 (2002)

Amendola, E., Carfagna, C., Giamberini, M., and Pisaniello, G., *Macromol. Chem. Phys.*, **196**, 1577 (1955)

Amendola, E., Carfagna, C., Giamberini, M., and Komitov, L., *Liquid Crystals*, **21**, 317 (1996)

Ampudia, J., Larrauri, E., Gil, E., Rodriguez, M., and Leon, L., *J. Appl. Polym. Sci.*, **71**, 1239 (1999)

Bai, S., Dotrong, M., Soloski, E., and Evers, R., *J. Polym. Sci: Part B: Polym. Phys.*, **29**, 119 (1991)

Barclay, G., Ober, C., Papathomas, K., and Wang, D., *J. Polym. Sci.: part A: Polym. Chem.* **30**, 1831 (1992a)

Barclay, G., McNamee, S., Ober, C., Papathomas, K., and Wang, D., *J. Polym. Sci.: part A: Polym. Chem.* **30**, 1845 (1992b)

Barton, J., and Shepherd, P., *Macromol. Chem.*, **176**, 919 (1975)

Benicewicz, B. C., and Hoyt, A. E., *U.S.Patent. 5, 114, 612* (1992)

Benicewicz, B., Smith, M., Langlois, D., Gavrin, A., and Douglas, E., *Polym. Prepr.*, **38**, 307 (1997a)

Benicewicz, B., Priester, R., Smith, M., Douglas, E., and Earls, J., *Chemtech.* 44(1997b)

Carfagna, C., Amendola, E., Giamberini, M., Filippov, A. G., and Bauer, R. S., *Liquid Crystals*. **13**, 571 (1993)

Carfagna, C., Amendola, E., and Giamberini, M., *Composite Structures*, **27**, 37 (1994a)

Carfagna, C., Amendola, E., and Giamberini, M., *J. Mat. Sci. Lett.*, **13**, 126 (1994b)

Carfagna, C., Nicolais, L., Amendola, E., Carfagna, C., Jr., and Filippov A. F., *J. Appl. Poly. Sci.*, **44**, 1465 (1992)

Dearlove, T., *J. Appl. Polym. Sci.* **14**, 1615 (1970)

de Gennes, P. G., *The physics of Liquid Crystals*, Oxford University Press: Belfast, Ireland (1974)

DeMeuse, M., Gillham, J., and Parodi, F., *J. Appl. Polym. Sci.* **64**, 15 (1997)

Dhar, P., *Computers and Chemistry,* **10**, 293 (1986)

Dodiuk, H., and Kenig, S., *Prog. Polym. Sci.*, **19**, 439 (1994)

Domszy, R., and Shannon, P., *Macromolecules*, **23**, 2790 (1990)

Douglas, E., Langlois, D., and Benicewicz, B., *Chem. Mater.*, **6**, 1925 (1994)

Dyakonov, T., Mann, P., Chen, Y., and Stevenson, W., *Polymer degradation and stability*, **54**, 67 (1996)

Earls, J. D., Hefner Jr., R. E., and Puckett, P. M., *US Patent, 5, 270,405* July 27 (1992)

Encyclopedia of polymer science and engineering 2nd edition, Wiley-Interscience (1986)

Enns, J., and Gillham, J., *J. Appl. Polym. Sci.*, **28**, 2567 (1983)

Farkas. A., and Strohm. P., *J. Appl. Polym. Sci*, **12**, 159 (1968)

Farren, C., Akatsuka, M., Takezawa, Y., and Itoh, Y., *Polymer*, **42**, 1507 (2001)

Feng, J., ph D dissertation, *Interaction and permeability of water with liquid crystalline thermoset* in Department of Materials Science and Engineering. 2001, University of Florida: Gainesville, FL.

Flory, P., *Principles of Polymer Chemistry*, Cornell university, Ithaca, N.Y, 1953

Flory, P. J., and Rona, G., *Mol. Cyst. Liz. Cryst*, **54**, 289 (1979)

Flynn, J., and Wal,. L., *Polym. Lett*, **4**, 323 (1966)

Frich, D., and Econom,. J., *J. Polym. Sci. Part A: Polym. Chem*, **35**, 1061 (1997)

Fukud,. T., Takada, A., Tsujii, Y., and Miyamoto, T., *Macromolecules*, **28**, 3387(1995)

Gao, J., Zhao, M., and Yang, L., *J. Appl. Polym. Sci.,* **63**, 1137 (1997)

Gavrin, A., Curts, C., and Douglas, E., *J. Polym. Sci: Part A: Polym. Chem*, **37**, 4184 (1999)

Gavrin, A., and Douglas, E., *Macromolecules*, **34**, 5876 (2001)

Giamberini, M., Amendola, E., and Carfagna, C., *Mol. Cryst. Liq. Cryst*, **266**, 9 (1995a)

Giamberin,. M., Amendola, E., and Carfagna, C., *Macromol. Rapid. Commun.*, **16**, 97 (1995b)

Gillham, J. K., and Enns, J. B., *TRIP*, **2**, 406 (1994)

Gouri, C., Reghunadhan Nair, C., Ramaswamy, R., and Ninan, K., *Eur. Polym. J.*, **38**, 503 (2002)

Han, S., Kim, W., Yoon, H., and Moon, T., *J. Appl. Polym. Sci.*, **68**, 1125 (1998)

Hikmet, R., and Broer. D., *Polymer*, **32**, 1627 (1991)

Hikmet, R. A. M., J. Lub and J. A Higgins, *Polymer*, **34**, 1736 (1993)

Horvath, I., Kranz, G., and Fedorenko, Y., *Reactivity of Solids,* **7**, 173 (1989)

Hoyt, A. E., Benicewicz, B., and Huang, S., *Polym. Preprints*, **30**, 536 (1989)

Hoyt, A. E., Benicewicz, B., and Huang, S., *ACS Symp. Series*, **435**, 198 (1990)

Hoyt, A. E., and Benicewicz, B., *J. Polym. Sci, Part A: Polym Chem*, **28**, 3403 (1990a)

Hoyt, A. E., and Benicewicz, B., *J. Polym. Sci, Part A: Polym Chem,* **28**, 3417 (1990b)

Hsu, T., Lin, Y., and Lee, Y., *J. Polym. Sci, Part A: Polym Chem*. **36**, 1791 (1998)

Jahromi, S., Kuipers, W. A. G., Norder, B., and Mijs, W.J., *Macromol*, **28**, 2201 (1995)

Jisova, V., *J. Appl. Polym. Sci*, **34**, 2547 (1987)

Kint, D., de Ilarduya, A., and Munoz-Guerra, S., *Polym. Prepr.,* **41**, 1209 (2000)

Körner, H., Shiota, A., Bunning, T., and Ober, C., *Science*, **272**, 252 (1996a)

Körner, H., Shiota, A., and Ober, C., *Liquid Crystal for advanced technologies Materials Research Society Symposium Proceedings*, **425**,149 (1996b)

Lam, J., Kong, X., Dong, Y., Cheuk, K., Xu, K., Tang, B., *Macromolecules*, **33**, 5027 (2000)

Lange, J., Altmann, N., Kelly, C., and Halley, P., *Polymer,* **41**, 5949 (2000)

Langlois, D., Benicewicz, B., and Douglas, E., *Chem. Mater*. **10**, 3393 (1998)

Laza, J., Julian, C., Larrauri, E., Rodriguez, M., and Leon, L., *Polymer*, **40**, 35 (1998)

Lee, J., and Jang, J., *Polym. Sci, Part A: Polym Chem.* **36**, 911 (1998a)

Lee, J., Jang, J., Hwang, S., Hong, S., and Kim, K., *Polymer*, **39**, 6121 (1998b)

Lee, J., Shim, J., and Kim, S., *J. Appl. Polym. Sci*., **81**, 479 (2001)

Liaw, D., and Shen, W., *Polym. Eng. and Sci*, **34**, 1297 (1994)

Lin, Q., Yee, A., Earls, J., Hefner Jr., R., and Sue, H., *Polymer*, **35**, 2679 (1994)

Lin, Q., Yee, A., Sue, H., Earls, J., and Hefner Jr., R., *J. Polym. Sci. Part B: Polym. Phys.*, **35**, 2363 (1997)

Lincoln, D., and Douglas, E., *Polym. Eng Sci.*, **39**, 1903 (1999)

Litt, M.H., Whang, W., Yen, K., and Quian, X., *J. Polym. Sci, Part A: Polym Chem*, **31,** 183 (1993)

Liu, J., Wang, C., and Campbell, G., *J. Eng. and Applied Science* **2,** 2417 (1996)

Liu, J., Wang, C., Campbell, G., Earls, J., and Priester. Jr., R., *J. Polym. Sci, Part A: Polym Chem.*, **35**, 1105 (1997)

Liu, Y., Zhao, M., Shen, S., and Gao, J., *J. Appl. Polym. Sci*, **70**, 1991 (1998)

Lu, M., Shim, M., and Kim, S., *J. Appl. Polym. Sci.,* **75**, 1514 (2000)

Mallon, J., and Adams, P. M., *J. Polym. Sci, Part A: Polym Chem.*, **31,** 2249 (1993)

Matějka, L., *Macromolecules*, **33**, 3611 (2000)

Mauri, A. N., Galego, N., Riccardi, C. C., and Williams, R., *Macromolecules*, **30,** 1616 (1997)

May, C. A., *Epoxy Resins: Chemistry and Technology,* 2nd ed., Marcel Dekker, inc., New York, 1988, chapter 13

Melissaris, A.P., and Litt, M.H., *Macromolecules,* **27,** 2675 (1994)

Micco, G., Giamberini, M., Amendola, E., Carfagna, C., and Astarita, G., *Ind. Eng. Chem. Res.*, **36,** 2976 (1997)

Mormann, W., and Zimmermann, J., *Macromolecules*, **29**, 1105 (1996)

Nam, J., and Seferis, J., *J. Appl. Polym. Sci. Part B: Polym. Phys.*, **29** 601 (1991)

Noel, C., and Navard, P., *Prog. Polym. Sci.*, **16**, 55 (1991)

Núñez, L., Fraga, F., Núñez, M. R., and Villanueva, M., *J. Appl. Polym. Sci.* **60**, 1931 (1991)

Núñez, L., Fraga, F., Núñez, M. R., and Villanueva, M., *J. Appl. Polym. Sci.* **70**, 1931 (1998)

Núñez, L., Taboada, J., Fraga, F., and Núñez, M. R., *J. Appl. Polym. Sci.*, **66**, 1377 (1997)

Ochi, M., Shimizu, Y., Nakanishi, Y., and Murata, Y., *J. Appl. Polym. Sci. Part B: Polym. Phys.*, **35**, 397 (1997)

Odian, G., *Principles of Polymerization* 3rd ed. John Wiley and Sons, Inc. (1991)

Ogawa, Y., *Polymer Journal*, **28**, 289 (1996)

Ooi, S., Cook, W., Simon, G., and Such, C., *Polymer*, **41**, 3639 (2000)

Oprea, S., *Polym. Deg. Stab.*, **75**, 9 (2002)

Ortiz, C., Belenky, L., Ober, C, and Kramer, E., *J. Mat. Sci.*, **35**, 2079 (2000)

Ortiz, C., Kim, R., Rodighiero, E., Ober, C, and Kramer, E., *Macromolecules*, **31**, 4074 (1998a)

Ortiz, C., Wagner, M., Bhargava, N., Ober, C, and Kramer, E., *Macromolecules*, **31**, 8531 (1998b)

Park, W. and Lee, J., *J. Appl. Polym. Sci*, **67**, 1101 (1998)

Penco, M., Sartore, L., Bignotti, F., D'Antone, S., and Di Landro, L., *Eur. Polym. J.*, **36**, 901 (2000)

Percec, V. and Lee, M., *Macromolecules*, **24**, 1017 (1991)

Pramoda, K., Chung, T., Liu, S., Oikawa, H., Yamaguchi, A., *Polym deg. and Stab.* **67**, 365 (2000)

Ricciardi F., Romanchick W. A., and Joullié M. M, *J. Polym. Sci, Part A: Polym Chem* **21**, 1475 (1983)

Satava, V., *Thermochimica Acta,* **2**, 423 (1971)

Scariah, K., Sekhar, V., and Rao, M., *Eur. Polym. J.* **30**, 925 (1994)

Shiota, A., Körner, H. and Ober, C., *Macromol. Chem. Phys.*, **198**, 2957 (1997a)

Shiota, A. and Ober, C., *Polymer*, **38**, 5857 (1997)

Shiota, A. and Ober, C. K., *Prog. Polym. Sci.*, **22**, 975 (1997b)

Simon, S. L. and Gillham, J., *J. Appl. Polym. Sci*, **46**, 1245 (1992)

Sperling, L. H., *Introduction to Physical Polymer Science* 2nd. Wiley, NY (1992)

Stockmayer, W. H., *J. Polym. Sci.*, **9**, 69 (1951)

Su, W-F., *Polym. Sci, Part A: Polym Chem,* **31**, 3251 (1993)

Tatsumiya, S., Yokokawa, K., and Miki, K., *J. Thermal Anal.*, **49**, 123 (1997)

Wang, X. and Gillham J., *J. Appl. Polym. Sci.*, **47** 425 (1993)

Wisanrakkit, G. and Gillham, J., *J. Coatings Technology*, **62**, 35 (1990)

Wyandt, C., and Flanagan, D., *Thermochimica Acta,* **197**, 239 (1992)

Yang, M., *Polym. Deg. Stab.,* **76**, 69 (2002)

Zentel, R., Strobl, G.R. and Ringsdorf, H., *Macromolecules*, **18**, 960 (1985)

Zukas, W., *J. Appl. Polym. Sci.*, **53**, 429 (1994)

BIOGRAPHICAL SKETCH

Seunghyun Cho was born in Seoul, Korea, on November 26, 1965. She was admitted to the Seoul National University in 1985, and there received her Bachelor of Science degree in Fiber and Polymer Engineering in 1989. She received her Master of Science degree in Fiber and Polymer Engineering from Seoul National University in 1991. Until she married Dr. Bongsoo Lee, she worked at a major polymer research lab in Daejon, Korea. They have a son, Chungwon Lee (born in 1993) and a daughter, Suyeon Lee (born in 2001). In 1997, she started her study toward a Doctor of Philosophy degree at the University of Florida in Gainesville, FL. Currently she is a candidate for the degree of Doctor of Philosophy in August 2002.

I certify that I have read this study and that in my opinion it conforms to acceptable standards of scholarly presentation and is fully adequate, in scope and quality, as a dissertation for the degree of Doctor of Philosophy.

Elliot P. Douglas, Chairman
Assistant Professor of Materials Science
and Engineering

I certify that I have read this study and that in my opinion it conforms to acceptable standards of scholarly presentation and is fully adequate, in scope and quality, as a dissertation for the degree of Doctor of Philosophy.

Ronald H. Baney
Associate Engineer, Materials Science
and Engineering

I certify that I have read this study and that in my opinion it conforms to acceptable standards of scholarly presentation and is fully adequate, in scope and quality, as a dissertation for the degree of Doctor of Philosophy.

Laurie A. Gower
Assistant Professor of Materials Science
and Engineering

I certify that I have read this study and that in my opinion it conforms to acceptable standards of scholarly presentation and is fully adequate, in scope and quality, as a dissertation for the degree of Doctor of Philosophy.

Wolfgang M. Sigmund
Associate Professor of Materials Science
and Engineering

I certify that I have read this study and that in my opinion it conforms to acceptable standards of scholarly presentation and is fully adequate, in scope and quality, as a dissertation for the degree of Doctor of Philosophy.

Randolph S. Duran
Associate Professor of Chemistry

This dissertation was submitted to the Graduate Faculty of the College of Engineering and to the Graduate School and was accepted as partial fulfillment of the requirements for the degree of Doctor of Philosophy

August, 2002

Pramod P. Khargonekar
Dean, College of Engineering

Winfred M. Phillips
Dean, Graduate School